JACS
JOURNAL OF THE AMERICAN CHEMICAL SOCIETY
Article
pubs.acs.org/JACS

Single-Step versus Stepwise Two-Electron Reduction of Polyarylpyridiniums: Insights from the Steric Switching of Redox Potential Compression

Jérôme Fortage,[†,‡] Cyril Peltier,[§] Christian Perruchot,[†] Yohei Takemoto,[∥] Yoshio Teki,[∥] Fethi Bedioui,[⊥] Valérie Marvaud,[‡] Grégory Dupeyre,[†] Lubomír Pospísil,[#] Carlo Adamo,[§] Magdaléna Hromadová,*[,#] Ilaria Ciofini,*[,§] and Philippe P. Lainé*[,†]

[†]Université Paris Diderot, Sorbonne Paris Cité, ITODYS, UMR 7086 CNRS, 15 rue Jean-Antoine de Baïf, 75013 Paris, France

[‡]UPMC, Université Paris 06, Institut Parisien de Chimie Moléculaire, UMR 7201 CNRS, Case 42, 4 place Jussieu, 75005 Paris, France

[§]École Nationale Supérieure de Chimie de Paris—Chimie ParisTech, LECIME, UMR 7575 CNRS, 11 rue Pierre et Marie Curie, 75005 Paris, France

[∥]Department of Material Science, Graduate School of Science, Osaka City University, 3-3-138 Sugimoto, Sumiyoshi-ku, Osaka 558-8585, Japan

[⊥]Université Paris Descartes, École Nationale Supérieure de Chimie de Paris—Chimie ParisTech, Laboratoire de Pharmacologie Chimique et Génétique et d'Imagerie, UMR 8151 CNRS and U 1022 INSERM, 11 rue Pierre et Marie Curie, 75005 Paris, France

[#]J. Heyrovsky Institute of Physical Chemistry, v.v.i., Academy of Sciences of the Czech Republic, Dolejskova 3, 18223 Prague, Czech Republic

Supporting Information

ABSTRACT: Contrary to 4,4′-dipyridinium (i.e., archetypal methyl viologen), which is reduced by two single-electron transfers (stepwise reduction), the 4,1′-dipyridinium isomer (so-called "head-to-tail" isomer) undergoes two electron transfers at apparently the same potential (single-step reduction). A combined theoretical and experimental study has been undertaken to establish that the latter electrochemical behavior, also observed for other polyarylpyridinium electrophores, is due to potential compression originating in a large structural rearrangement. Three series of branched expanded pyridiniums (EPs) were prepared: *N*-aryl-2,4,6-triphenylpyridiniums (Ar-**TP**), *N*-aryl-2,3,4,5,6-pentaphenylpyridiniums (Ar-**XP**), and *N*-aryl-3,5-dimethyl-2,4,6-triphenylpyridinium (Ar-**DMTP**). The intramolecular steric strain was tuned via *N*-pyridinio aryl group (Ar) phenyl (Ph), 4-pyridyl (Py), and 4-pyridylium (qPy) and their bulky 3,5-dimethyl counterparts, xylyl (Xy), lutidyl (Lu), and lutidylium (qLu), respectively. Ferrocenyl subunits as internal redox references were covalently appended to representative electrophores in order to count the electrons involved in EP-centered reduction processes. Depending on the steric constraint around the *N*-pyridinio site, the two-electron reduction is single-step (Ar = Ph, Py, qPy) or stepwise (Ar = Xy, Lu, qLu). This steric switching of the potential compression is accurately accounted for by ab initio modeling (Density Functional Theory, DFT) that proposes a mechanism for pyramidalization of the $N_{pyridinio}$ atom coupled with reduction. When the hybridization change of this atom is hindered (Ar = Xy, Lu, qLu), the first reduction is a one-electron process. Theory also reveals that the single-step two-electron reduction involves couples of redox isomers (electromers) displaying both the axial geometry of native EPs and the pyramidalized geometry of doubly reduced EPs. This picture is confirmed by a combined UV−vis−NIR spectroelectrochemical and time-dependent DFT study: comparison of in situ spectroelectrochemical data with the calculated electronic transitions makes it possible to both evidence the distortion and identify the predicted electromers, which play decisive roles in the electron-transfer mechanism. Last, this mechanism is further supported by in-depth analysis of the electronic structures of electrophores in their various reduction states (including electromeric forms).

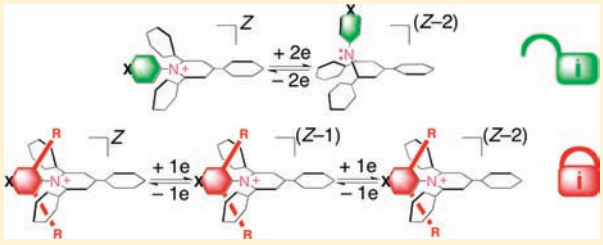

1. INTRODUCTION

At the nanoscale, and more specifically at the (intra)molecular level, manipulating several electrons at the same time remains a highly challenging task.[1] In fact, this constitutes a goal of utmost importance in the related fields of molecular electronics[2] and artificial photosynthesis,[3] among others. Therefore, there exists a real interest in gaining insights into

Received: October 25, 2011
Published: December 25, 2011

   dx.doi.org/10.1021/ja210024y | J. Am. Chem.Soc. 2012, 134, 2691−2705

the manner by which certain redox-active molecules (in particular, reducible electrophores) can handle multielectron processes not only with respect to through-bond (electronic) and through-space (electrostatic) interactions[4−6] but also by adapting their architecture.[7,8] In this context, we have undertaken the in-depth study of a series of pyridinium-based model electrophores, hereafter referred to as branched expanded pyridiniums (EPs).[9−11] These EPs are capable of undergoing multiple reduction processes in different manners, and the unraveling of their peculiar structure−electrochemistry relationships is ultimately expected to lead to a potentially workable principle for electron storage.[12−15]

At the (intra)molecular level, as far as semirigid and potentially fully conjugated systems are concerned, the relationships between structure (more specifically conformation) and the dynamics of electron transfers, as well as intercomponent electronic coupling, are well established.[16,17] A typical instance is the conformational gating of photoinduced processes within two-component systems conceived for charge separation.[18] The electrochemical properties of molecular electrophores can also be varied conformationally, provided that they have roughly the same intramolecular characteristics as above. This is illustrated by the benchmark case of bipyridinium isomers and derivatives (viologen-like species), when the torsion angle about their interannular linkage is gradually changed.[19] Thereby, the critical energy of their lowest unoccupied molecular orbital (LUMO), that governs their reduction processes, is steadily changed. Only mild tuning of electrochemical behavior is obtained in this way: the number of electrons exchanged remains the same and the standard potential(s) is(are) moderately shifted.[20] In a further step of molecular design, one may ask whether the redox properties and, more specifically, the *reduction regime* of electrophores can be *drastically changed* by structural factors, such as intramolecular steric hindrance.[21] Achieving genuine steric switching of electronic landscapes, giving rise to two distinguishable states with totally different electrochemical features, would be the target.[22] The underlying working principle would rely on a sterically controlled upheaval of redox-active molecular orbitals (MOs) arising either from their very nature or from the way in which incoming electron density is distributed among them (case of redox isomers or electromers[23]).

Because of their great chemical versatility, combined with the possibility of multielectron reduction, polyarylpyridinium electrophores of the branched EP type[9−11] offer a unique opportunity to explore such structure−property relationships. In this respect, the intriguing observation that the *N*-pyridylium-2,4,6-triphenylpyridinium electrophore (qPy-**TP**) is two-electron-reduced in a single-step process at −0.60 V (vs SCE, in MeCN)[11] merits our attention. The following question arises: how can these two electrons be added at apparently the same potential to such a small compact semirigid electrophore, and the electrostatic (i.e., Coulombic) repulsion be overcome? Indeed, except for metal ions, (single-step) multielectron reduction is known to occur essentially in two ways: (1) The redox-active sites do not experience electrostatic interaction; however, in view of the molecular structures, this explanation can reasonably be ruled out here. (2) There is an electrostatic interaction but the system adapts to minimize it via a structural rearrangement[8] or by counterbalancing adverse repulsion with some gain in electronic stability (e.g., resonance energy/aromaticity).[24] The second reduction thus becomes as easy as (case a) or even easier than (case b) the first one. This phenomenon, known as "potential compression" (case a) or "potential inversion" (case b),[8] is clearly the more likely. More precisely, pyramidalization of the $N_{pyridinio}$ atom of the pyridinium core, originating from a change in its hybridization during reduction, is postulated (Figure 1).[11]

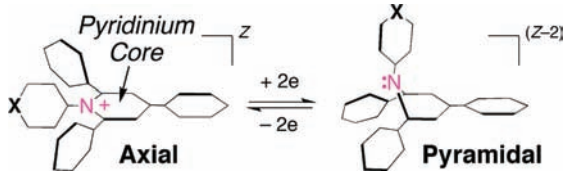

Figure 1. Pictorial representation of the type of structural distortion assumed in the potential compression/inversion. X = CH, N, or N^+-Me, and *Z* is the charge of the electrophore in its native form (*Z* = 1+, 2+).

The existence of such a redox-driven structural upheaval is primarily inferred on the basis of a computational study on the two-electron-reduced hexaphenylpyridinium (Ph-**XP**).[9] It also comes from spectroscopic (Raman)[25a] and theoretical[25b] work on the singlet-excited charge-transfer state of pyridinium-*N*-phenolate betaine, B30. The present work aims to ascertain the reality of this distortion (Figure 1) and to demonstrate that it plays a critical role in the two-electron reduction of branched EPs. This demonstration is based on a synthetic strategy conceived to take advantage of the impact of intramolecular steric hindrance on the reduction behavior. Thus, we propose the mechanism by which the ability of some electrophores to store one or two electron(s) at a given potential is switched. In the following, we refer to "two elementary electron transfers that occur apparently at the same potential" as a "single-step two-electron" reaction.

2. MOLECULAR DESIGN AND METHODOLOGICAL APPROACH

Comparison of the electrochemical behaviors of two-component systems (dyads in Figure 2) consisting of a ferrocenyl moiety (Fc) covalently linked via a phenylene spacer to a *N*-methyl-2,4,6-triphenylpyridinium (Me-**TP**) or a 1,2,4,6-tetraphenylpyridinium (Ph-**TP**) moiety affords a first indication that there might be interplay between steric hindrance and the reduction processes within branched EPs.

A dramatic shrinking of the potential difference (ΔE) related to the one-electron reductions is observed on going from Me-**TP** (ΔE = 460 mV)[11] to Ph-**TP** (ΔE = 160 mV),[9] that is, on replacing the methyl by an aryl group like phenyl at the $N_{pyridinio}$ atom. To what extent this change of electrochemical behavior is related purely to steric strain or whether there are also electronic factors is one of the issues addressed here.

Our approach for unraveling the precise nature of structure−property relationships within branched EPs relies on the steady increase in the intramolecular crowding to produce steric gating of the reduction regimes (two single-electron transfers versus one two-electron process).[26] The model electrophores synthesized for this purpose are depicted in Chart 1 (see also Supporting Information).[27]

Two types of steric constraint are systematically varied. On one hand, the *N*-pyridinio aryl group (Ar) linkage is encumbered by inserting methyls (R = H becomes R = Me to give Ar = Ph/Xy, Py/Lu, and qPy/qLu; Chart 1) to lock the electrophores in their axial conformation and, to some extent,

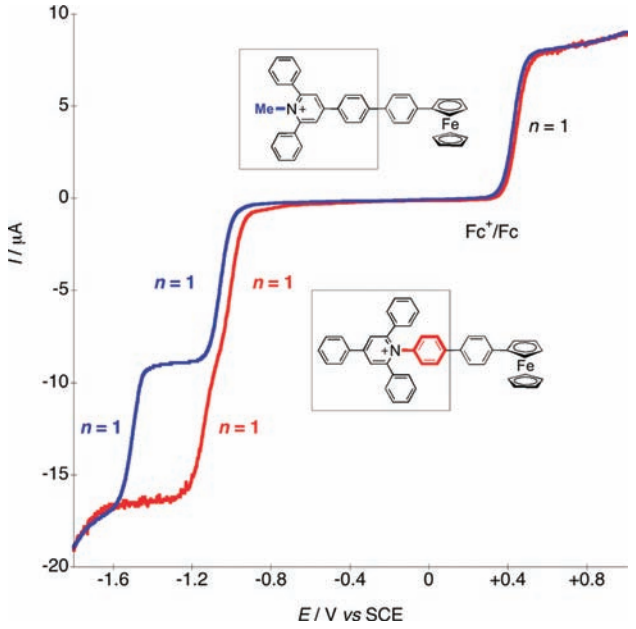

Figure 2. Appending an aryl group at the *N*-pyridinio position of EPs. Rotating disk electrode (RDE) voltammetry illustrates the impact on electrochemical features (potential compression): superimposed RDE voltammogram traces of Fc-based dyads related to Me-**TP** and Ph-**TP**, normalized with respect to one-electron redox process of Fc^+/Fc couple as internal reference (solvent is acetonitrile, MeCN).

Chart 1. Changing Intramolecular Steric Strain within Branched EPs while Counting the Electrons Involved in Reduction Processes[a]

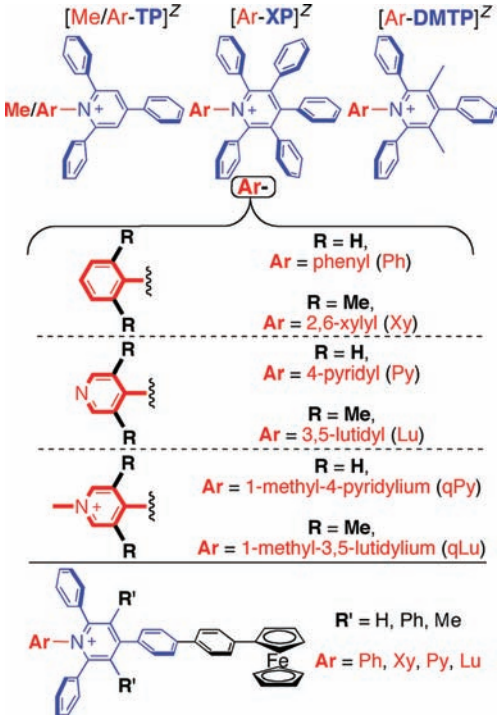

[a]Molecular structures and related labels of the tetraaryl- (**TP**), hexaaryl- (**XP**), and mixed-branched 3,5-dimethyl-**TP** (**DMTP**) pyridiniums synthesized and studied. *Z* is the electrophore charge in its native form. Counteranions are BF_4^- for monocationic EPs (Z = 1+) and PF_6^- for dicationic EPs (Z = 2+).

block pyramidalization (Figure 1). On the other hand, the bulkiness of the pyridinium core is steadily increased by changing its β substituents R′ (i.e., H, Ph, and Me at positions 3 and 5), to give electrophores of types Ar-**TP**, Ar-**XP**, and Ar-**DMTP**, respectively (Chart 1). This type of structural modification is aimed at changing the energy barrier between axial and pyramidal configurations and/or their relative stabilities. Last, selected electrophores are derivatized with a ferrocenyl group as an internal redox probe (one-electron oxidation process related to the Fc^+/Fc couple) to count the number of electrons involved in each process.[28,29] Syntheses and full characterization of model electrophores and dyads are given in the Supporting Information.

3. RESULTS AND DISCUSSION

3.1. Interplay between Structure and Electrochemical Properties: Insights from Theory. We start with the results of the initial molecular modeling study, carried out to rationalize the already reported experimental findings, especially those of the **TP** series bearing a *N*-pyridinio aryl group lacking methyl substituents (Ar = Ph, Py, and qPy; Chart 1).[9,11] Geometry optimization was performed for the electrophores in their native state ($[\mathbf{TP}]^Z$) as well as for their singly ($[\mathbf{TP}]^{(Z-1)}$) and doubly ($[\mathbf{TP}]^{(Z-2)}$) reduced states, prior to calculating the standard potentials for their first and second reductions. The geometries obtained differ essentially in the torsion angles only (in particular the interannular Ar—pyridinium angle), which were found to decrease upon reduction (planarization). We shall refer to these geometries as *axial* (Figure 1). If these computed structures are not surprising as such,[18] they clearly do not conform to our above-stated expectations (Figure 1) of an emerging pyramidalization of the $N_{pyridinio}$ atom giving rise to *distorted* structures, referred to as *pyramidal* structures (Figure 1), at least for what concerns the doubly reduced species. Furthermore, the computed reduction potentials ($E([\mathbf{TP}]^{Z/(Z-1)})$ and $E([\mathbf{TP}]^{(Z-1)/(Z-2)})$) were found to be very different. This finding is in contradiction with the experimental observation of two very close one-electron reductions (Ar = Ph, Figure 2)[9] or even of an apparent two-electron process (Ar = Py and qPy).[11]

On the other hand, for the crowded **XP** series (Chart 1) bearing the same Ar groups without methyl substituents, like Ph[9] or Py and qPy (present work), structure optimization of the doubly reduced electrophores ($[\mathbf{XP}]^{(Z-2)}$) yielded a single minimum corresponding to a pyramidalized geometry (Figure 3; Table S1 in Supporting Information). In other words, the axial form of $[\mathbf{XP}]^{(Z-2)}$ is unstable. Interestingly, for these **XP** types of electrophores in their singly reduced state ($[\mathbf{XP}]^{(Z-1)}$), geometry optimization leads to axial structures ($[\mathbf{XP}(\text{axial})]^{(Z-1)}$) when one starts from their native axial geometry (i.e., $[\mathbf{XP}(\text{axial})]^Z$ + 1 electron), whereas pyramidal structures ($[\mathbf{XP}(\text{pyramid})]^{(Z-1)}$) are obtained from the pyramidalized geometry of the doubly reduced electron acceptors (i.e., $[\mathbf{XP}(\text{pyramid})]^{(Z-2)}$ − 1 electron), as schematized in Figure 3. This finding is a strong indication that there are at least two wells (minima) in the potential energy surface (PES), i.e., two possible forms for the one-electron-reduced **XP** electrophores ($[\mathbf{XP}]^{(Z-1)}$), namely $[\mathbf{XP}(\text{axial})]^{(Z-1)}$ and $[\mathbf{XP}(\text{pyramid})]^{(Z-1)}$. These redox isomers are referred to as electromers.[23] Moreover, if it is assumed that $[\mathbf{XP}(\text{axial})]^{(Z-1)}$ electromers are the relevant intermediates, the reduction potentials ($E([\mathbf{XP}]^{Z/(Z-1)})$ and $E([\mathbf{XP}]^{(Z-1)/(Z-2)})$) are found to be almost equal (within ca. 0.1 V) in the cases of Ar = Ph, Py,

dx.doi.org/10.1021/ja210024y | J. Am. Chem.Soc. 2012, 134, 2691−2705

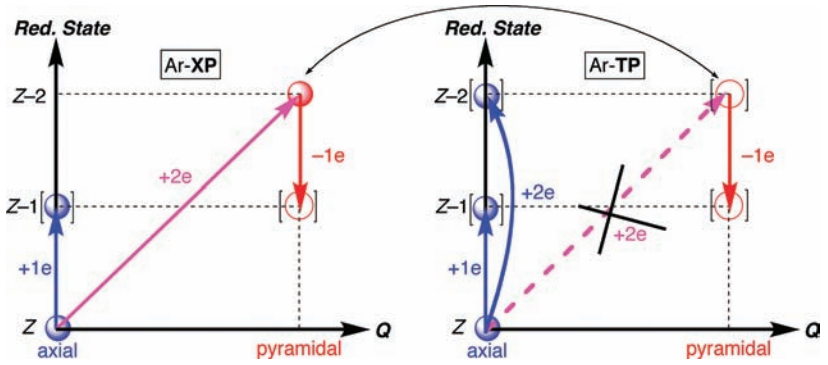

Figure 3. Perfecting the computational procedure (geometry optimization) for Ar-**XP** and Ar-**TP** with Ar = Ph, Py, and qPy. Coordinate Q represents the structural form of the electrophore for a given reduction state: "axial" or "pyramidal". Closed circles indicate optimized structures directly obtained from the native forms upon electron addition, whereas open circles denote optimized geometries derived from pyramidalized doubly reduced forms. Redox isomers (electromers) are in brackets.

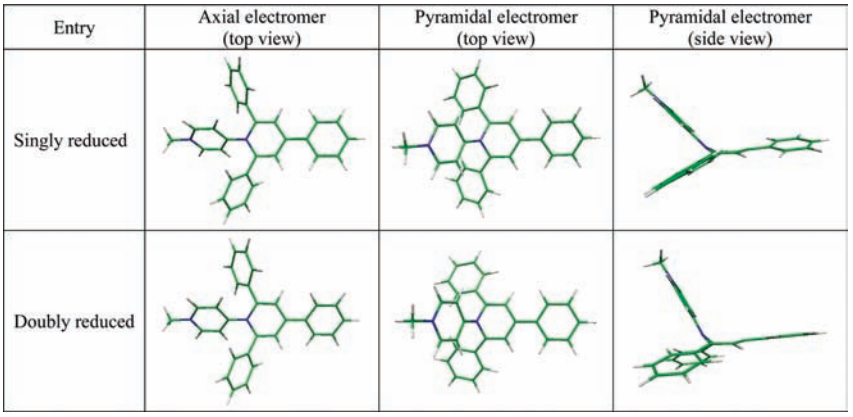

Figure 4. Optimized molecular geometries for the singly and doubly reduced forms of Ar-**TP**-type electrophores (representative case of Ar = qPy). Pathways to $[\mathbf{TP}(\text{pyramid})]^{(Z-2)}$ involving $[\mathbf{TP}(\text{axial})]^{(Z-1)}$ or $[\mathbf{TP}(\text{pyramid})]^{(Z-1)}$ as intermediates are equally relevant.

and qPy[30] ("potential compression"; Table S1), in line with the experimental single-step two-electron reductions (see section 3.2 below and ref 9). Note that the assumption that $[\mathbf{XP}(\text{pyramid})]^{(Z-1)}$ electromers are involved also leads to almost equal values of potentials for these aryl groups, but with the second reduction more anodic than the first one ("potential inversion"[30]), which also accounts well for the electrochemical measurements. While electrochemistry does not discriminate clearly between the two options, strict interpretation of the computational results (Table S1), however, suggests that the more likely explanation is a slight inversion of potential (see section 3.2 below).

Most important, here, is the fact that the consistency of the theoretical and experimental findings for the Ar-**XP** series (with Ar = Ph, Py, and qPy) relies on the assumption of an intervening pyramidalized structure, at least for doubly reduced species, hence the idea of considering this possibility for electrophores of the **TP** series (Figures 1 and 2). Thus, when this particular distortion was introduced into our computational approach (Figure 3), the pyramidal geometries were indeed found to correspond to real energy minima for both the singly and the doubly reduced Ar-**TP** electrophores (Ar = Ph, Py, and qPy; Figures 3 and 4; Table S2 in Supporting Information). Also, similar values for reduction potentials ($E([\mathbf{TP}]^{Z/(Z-1)})$ and $E([\mathbf{TP}]^{(Z-1)/(Z-2)})$) were derived (Table S2), this time in accordance with experimental findings.[9,11]

This computational approach was therefore applied (Experimental Section) to assess the reduction potentials of each of the 19 electrophores depicted in Chart 1, thus exploring systematically axial and pyramidal geometries for singly and doubly reduced species. All calculated data are collected in Tables S1–S3 (Supporting Information).

3.2. Reduction Behavior of Branched EPs: Combined Electrochemical and Theoretical Study. Parallel to the theoretical study, the electrochemical behavior of the whole series of electrophores and dyads (Chart 1) was investigated by potentiodynamic methods including cyclic voltammetry (CV) and hydrodynamic experiments (rotating disk electrode (RDE) voltammetry). Table 1 lists the data (see also Supporting Information).

Two main trends can be seen. On one hand, when the aryl group at the *N*-pyridinio position of the pyridinium core is sterically demanding (i.e., Ar = Xy, Lu, and qLu; Chart 1), the first reduction process involves one electron. This process is most often reversible (the only exception is qLu-**DMTP**), regardless of the level of steric constraint in the periphery of the pyridinium platform (**TP**, **XP**, or **DMTP**; see Figure 5a,c and Supporting Information). When the second one-electron reduction is observed (**TP** series; see Supporting Information), the process occurs at much higher potential and is systematically irreversible. On the other hand, when the aryl group has no bulky substituent (i.e., Ar = Ph, Py, and qPy), the first reduction process always involves two electrons (see Figure 5c and Supporting Information) and its reversibility is sensitive to the degree of crowding of the pyridinium platform (reversible or irreversible; see Figure 5b and Supporting Information).

dx.doi.org/10.1021/ja210024y | J. Am. Chem.Soc. 2012, 134, 2691–2705

Table 1. Reduction of Model Electrophores[a] and Ferrocenyl-Based Dyads (Chart 1) at Pt Electrode (vs SCE) for MeCN Solutions (+0.1 M NBu_4PF_6) at Room Temperature[b]

entry	$E_{1/2}$, V	n	$E_{1/2}$, V	n
Me-**TP**[c]	−1.07; rev.	1	−1.53; rev.	1
Ph-**TP**[d]	−1.00; rev.	1	−1.16; rev.	1
Xy-**TP**	−1.06; rev.	1	−1.83 (E_{pc}); irrev.	1
Py-**TP**[c]	−0.93; rev.	2		
Lu-**TP**	−0.92; rev.	1	−1.70; irrev.	1
qPy-**TP**[c]	−0.60; rev.	2		
qLu-**TP**	−0.70; rev.	1	−1.23 (E_{pc}); irrev.	1
Ph-**XP**[d]	−1.17[e]; quasi-rev.	2		
Xy-**XP**	−1.16; rev.	1	[f]	
Py-**XP**	−1.10 (E_{pc}); irrev.	2		
qPy-**XP**	−0.73 (E_{pc}); irrev.	2		
Ph-**DMTP**	−1.33 (E_{pc}); irrev.	$1 < n < 2$[g]		
Xy-**DMTP**	−1.30; rev.	1	[f]	
Py-**DMTP**	−1.20; quasi-rev.	2		
Lu-**DMTP**[h]	−1.23; rev.	1	[f]	
qPy-**DMTP**	−0.84 (E_{pc}); irrev.	2		
qLu-**DMTP**	−0.93 (E_{pc}); irrev.	1	−1.40 (E_{pc}); irrev.	1

[a]With the exception of Lu-**XP** and qLu-**XP**: see ref 27. [b]Unless otherwise noted, $E_{1/2}$ (vs SCE) is calculated as $(E_{pa} + E_{pc})/2$, where E_{pa} and E_{pc} are anodic and cathodic peak potentials measured by CV at 0.1 V s^{-1}; n is the number of electrons involved in the redox process determined by RDE voltammetry with Fc-based dyads (see text). For more details, see Experimental Section. [c]From ref 11. [d]From ref 9. [e]E_{pc}. [f]Beyond the investigated potential window (below −1.90 V). [g]See refs 31 and 32. [h]From the corresponding Fc-based dyad.

Note that the electrophore Ph-**TP** is a borderline case, since two partly merged one-electron waves are observed instead of a single two-electron wave (Figure 2).

The overall picture we get from the CV and RDE results (see also Supporting Information), is the following: other things being equal, *the one- or two-electron nature of the first reduction process is solely governed by the bulkiness of the N-pyridinio aryl group*. This picture is fully consistent with the assumption that *N*-pyramidalization during reduction is responsible for the potential compression (or inversion), which naturally vanishes when it is prevented by steric hindrance of the aryl group.

As regards two-electron processes (Ar = Ph, Py, and qPy), the relative degrees of reversibility/irreversibility depend on steric parameters essentially varied via the β substituents on the pyridinium core (Chart 1). Clearly, the reversibility is more pronounced when there is more room for intramolecular structural rearrangement. From the theoretical viewpoint, as far as singly reduced species are concerned, both axial and pyramidal electromeric structures are minima in the PES (Figures 3 and 4 and Supporting Information). The same also holds for the **XP** and **DMTP** series (Tables S1 and S3). For the **TP** series, these electromers have similar stabilities (Table S2). Regarding doubly reduced species, the two types of electromeric structures are found by calculation only in the case of the **TP** family. For all three families (**TP**, **XP**, and **DMTP**), the pyramidal structures are found to be by far the more stable (Tables S1−S3). Clearly, the most likely explanation for the different degrees of reversibility of two-electron reductions is twofold: (1) different stabilities for the two singly reduced electromers with respect to that of the final pyramidalized doubly reduced species and (2) different interconversion energy barrier heights.[34]

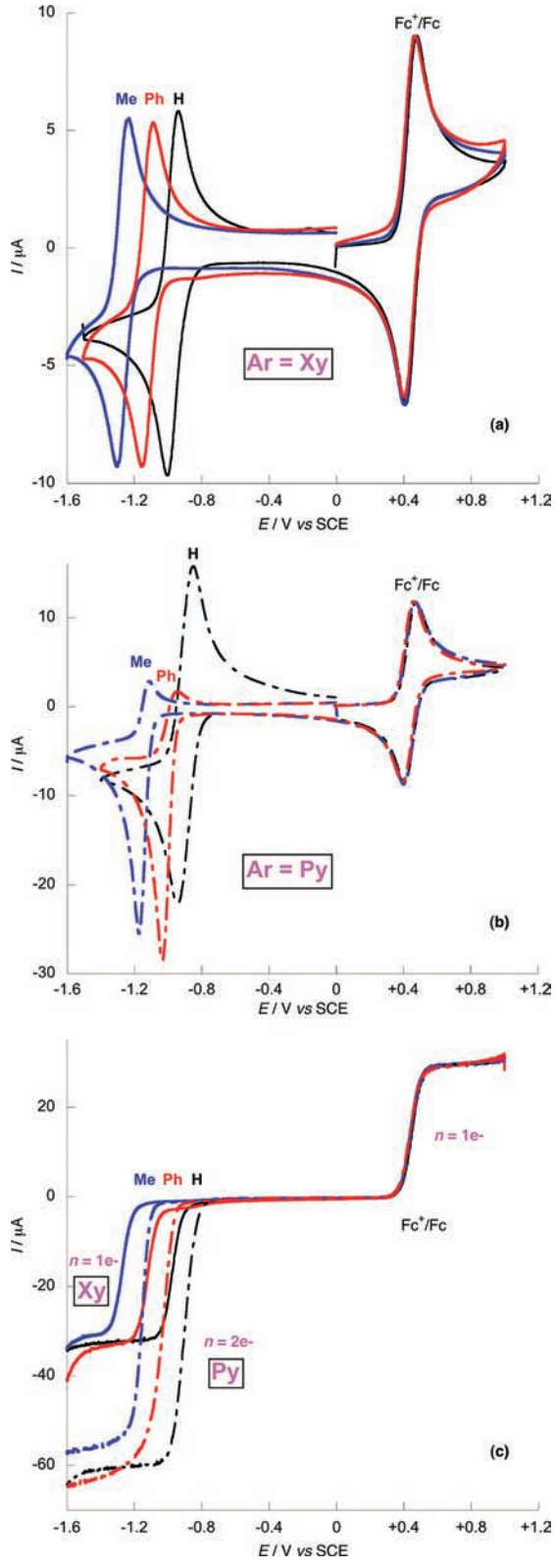

Figure 5. Impact of various steric constraints on electrochemical features.[33] Superimposed representative voltammograms of Fc-based dyads containing Ar-**TP** (R′ = H; black), Ar-**XP** (R′ = Ph; red), and Ar-**DMTP** (R′ = Me; blue). (a) CV, Ar = Xy. (b) CV, Ar = Py. (c) RDE voltammetry, Ar = Xy (solid lines) and Py (dashed-dotted lines). Plots of dyads are normalized with respect to the one-electron redox process of the Fc^+/Fc couple.

Concerning one-electron processes (Ar = Xy, Lu, and qLu), the reversibility of the first reduction is in line with the slight

dx.doi.org/10.1021/ja210024y | J. Am. Chem.Soc. 2012, 134, 2691−2705

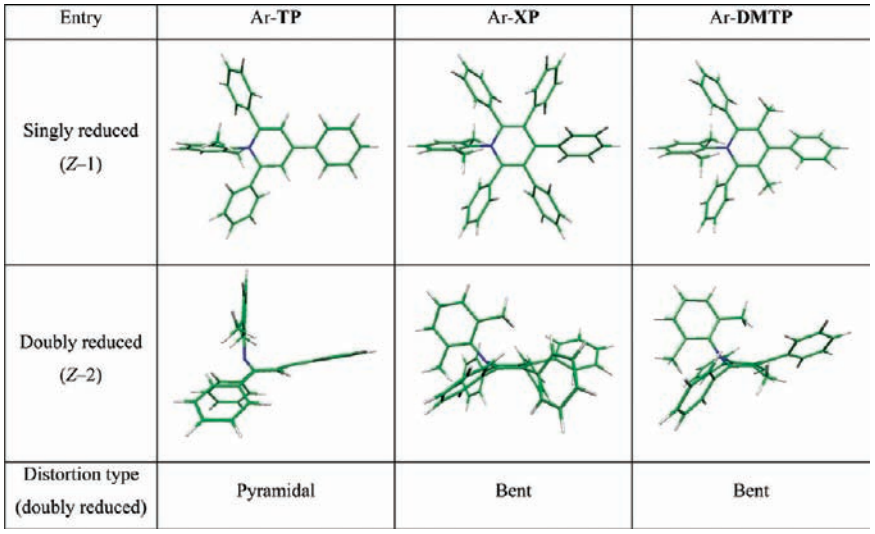

Figure 6. Representative optimized molecular geometries for the singly (top) and doubly (bottom) reduced forms of electrophores Ar-**TP**, Ar-**XP**, and Ar-**DMTP** (representative case of Ar = Xy).

conformational changes computed for the one-electron-reduced electrophores with bulky aryl groups. They all show an axial structure closely resembling that of their native forms as the only minimum of the PES (see Figure 6 and Tables S1−S3). The systematic irreversibility of the second one-electron reduction, when observed (only in the case of the **TP** series), can be explained by the unexpected formation of the severely and even locked *pyramidalized* structures computed for the doubly reduced species (see Supporting Information and Table S2[30]). Less severely distorted structures, referred to as *bent* structures (onset *N*-pyramidalization), are also computed as the only stable products for the more sterically crowded doubly reduced **XP** and **DMTP** (Figure 6). In all cases, the driving force for the change of hybridization of the $N_{pyridinio}$ atom is apparently sufficiently strong to overcome the steric hindrance produced by the Me substituents of the aryl group (Ar = Xy, Lu, and qLu).

To summarize, from this combined electrochemical and theoretical study, one can derive the redox equations that account accurately for the two observed reduction behaviors.

As regards the single-step two-electron reduction ("*compression* of potential", $\Delta E > 0$ with ΔE approaching 0, or "*inversion* of potential", $\Delta E(\text{theory}) \leq 0$ but $\Delta E(\text{exptl}) = 0$, see Tables 1 and S1−S3)[8] of branched expanded pyridiniums (**EP**):

$$[\mathbf{EP}(\text{axial})]^{Z} \xrightarrow{+e} [\mathbf{EP}^{\bullet}(\text{axial})/\mathbf{EP}^{\bullet}(\text{pyramid})]^{(Z-1)} \qquad E_1 \qquad (1)$$

$$[\mathbf{EP}^{\bullet}(\text{axial})/\mathbf{EP}^{\bullet}(\text{pyramid})]^{(Z-1)} \xrightarrow{+e} [\mathbf{EP}(\text{pyramid})]^{(Z-2)} \qquad E_2 \qquad (2)$$

Disproportionation:

$$2[\mathbf{EP}^{\bullet}(\text{axial/pyramid})]^{(Z-1)} \rightleftharpoons [\mathbf{EP}(\text{pyramid})]^{(Z-2)} + [\mathbf{EP}(\text{axial})]^{Z}$$

$$\Delta E = E_2 - E_1 \qquad (3)$$

Calculations tell us that the two types of electromers, $[\mathbf{EP}^{\bullet}(\text{axial})]^{(Z-1)}$ and $[\mathbf{EP}^{\bullet}(\text{pyramid})]^{(Z-1)}$, are roughly isoenergetic for Ar = Ph, Py, and qPy (see Tables S1−S3). As regards the net electrochemical−distortion−electrochemical process (herein referred to as an ECE process) related to the single-step two-electron reduction, the question is now raised as to whether the distortion is concerted[35,36] with the first elementary one-electron reduction or if the two electromers interconvert after the first reduction. In the latter case, the situation is as follows:

$$[\mathbf{EP}(\text{axial})]^{Z} \xrightarrow{+e} [\mathbf{EP}^{\bullet}(\text{axial})]^{(Z-1)} \qquad E_1 \qquad (4)$$

$$[\mathbf{EP}^{\bullet}(\text{axial})]^{(Z-1)} \rightleftharpoons [\mathbf{EP}^{\bullet}(\text{pyramid})]^{(Z-1)} \qquad \text{Interconversion} \qquad (5)$$

$$[\mathbf{EP}^{\bullet}(\text{pyramid})]^{(Z-1)} \xrightarrow{+e} [\mathbf{EP}(\text{pyramid})]^{(Z-2)} \qquad E_2 \qquad (6)$$

Then, as the pyramidalized doubly reduced electrophore is by far the more stable, the electromer adopting this structure ($[\mathbf{EP}^{\bullet}(\text{pyramid})]^{(Z-1)}$) is therefore readily reduced, hence the rapid consumption of $[\mathbf{EP}^{\bullet}(\text{axial})]^{(Z-1)}$. This is reflected by the disproportionation constant, which indicates that one-electron-reduced electrophores are unstable. In the case of electron acceptors of the **TP** type, contrary to **XP** and **DMTP** types of electrophore, calculations indicate that the axial doubly reduced electromers ($[\mathbf{EP}(\text{axial})]^{(Z-2)}$) also exist despite being much less stable than the pyramidal ones, $[\mathbf{EP}(\text{pyramid})]^{(Z-2)}$ (Table S2). This opens up the possibility of another interconversion equilibrium between electromers, this time involving $[\mathbf{EP}(\text{pyramid})]^{(Z-2)}$ and $[\mathbf{EP}(\text{axial})]^{(Z-2)}$, although highly unfavorably displaced for the latter. This second interconversion process, along with the previous one, reflects the moderate steric strain present within Ar-**TP** electrophores. Both equilibria are consistent with the observed reversibility of two-electron reduction when Ar = Ph, Py, and qPy (Table 1, Figure 5b, and Supporting Information). Overall, the postulated fluxional behavior[32] related to the existence of electromers and interconversion equilibria (eqs 4−6) appears as the most likely explanation for the observed reduction behaviors, and is therefore preferred to a hypothetical distortion concerted

dx.doi.org/10.1021/ja210024y | *J. Am. Chem.Soc.* 2012, 134, 2691−2705

with the first one-electron exchange, resembling that observed in nitroalkanes, for instance.[36,37] Based on computational results, it follows that the single-step two-electron reduction can be explained by a *compression* of potential in the case of **TP** type electrophores (Table S2) and by an *inversion* of potential for **XP** electrophores (Table S1). In the case of the **DMTP** series, one can hardly decide between compression or inversion of potential (Table S3).

Concerning the stepwise two-electron reduction (two successive one-electron processes: $\Delta E > 0$) within branched EPs with Ar = Xy, Lu, and qLu, the computational study reveals that there is no couple of electromers for the singly reduced electrophores (see Tables S1−S3); hence, there is no possible interconversion equilibrium. Consequently, the change of hybridization is most likely concerted with the second one-electron reduction.

$$[\mathbf{EP}(\text{axial})]^{Z} \xrightarrow{+e} [\mathbf{EP}^{\bullet}(\text{axial})]^{(Z-1)} \qquad E_1 \qquad (4)$$

$$[\mathbf{EP}^{\bullet}(\text{axial})]^{(Z-1)} \xrightarrow{+e} [\mathbf{EP}(\text{pyramid})]^{(Z-2)} \qquad E_2 \qquad (7)$$

3.3. Electrochromic Behavior of Branched EPs: Combined Spectroelectrochemical and Theoretical Study. UV−vis−NIR spectroelectrochemistry is the method of choice for probing the identity of the reduced species formed in solution during potentiodynamic measurements. For an electrophore of a given reduction state (i.e., native, singly reduced, or doubly reduced), different spectral signatures are expected for its axial and pyramidal structures (if they exist), based upon their differently extended π-delocalized systems. Three representative electrophores of the **TP**-type were investigated (Chart 1): Me-**TP** (Figure 7), qPy-**TP** (Figure 8), and qLu-**TP** (Figure 9). In Figures 7−9 are superimposed experimental plots and the calculated electronic transitions (time-dependent DFT (TD-DFT) results; Supporting Information, Tables S5−S7) corresponding to the forms (axial or pyramidal) that match the experimental results. For the sake of clarity, calculated transitions for the forms of reduced electrophores that do not match the experimental spectra are given in Supporting Information (Figures S2−S4).

In spite of the fact that energies of electronic transitions calculated by our approach (Tables S5−S7) are often slightly overestimated, they are in the range of accuracy expected for the level of theory used[39] and they reflect the experimental spectra.

In the case of Me-**TP**, the structure optimizations performed on the axial forms for both the one-electron and the two-electron-reduced species all converge to the pyramidalized geometry. Consequently, electronic transitions corresponding only to the three chromophoric species are reported (Figure 7): the axial native form, $[\text{Me-}\mathbf{TP}]^{+}$, and the one- and two-electron-reduced pyramidal forms, $[\text{Me-}\mathbf{TP}]^{0}$ and $[\text{Me-}\mathbf{TP}]^{-}$, respectively. The good agreement between experiment and theory at the TD-DFT level (Figures 7 and S5) further supports our inferences concerning Me-**TP**, and validates our present approach.

In the case of qPy-**TP**, whether in its singly or doubly reduced form, both the pyramidal and the axial redox isomers correspond to minima on the PES. Therefore, the features of up to five chromophoric species were calculated: $[\text{qPy-}\mathbf{TP}(\text{axial})]^{2+}$, $[\text{qPy-}\mathbf{TP}(\text{axial})]^{+}$, $[\text{qPy-}\mathbf{TP}(\text{pyramid})]^{+}$, $[\text{qPy-}\mathbf{TP}(\text{axial})]^{0}$, and $[\text{qPy-}\mathbf{TP}(\text{pyramid})]^{0}$ (Table S6). Apart from the $[\text{qPy-}\mathbf{TP}]^{2+}$ native electrophore, the calculated pattern of

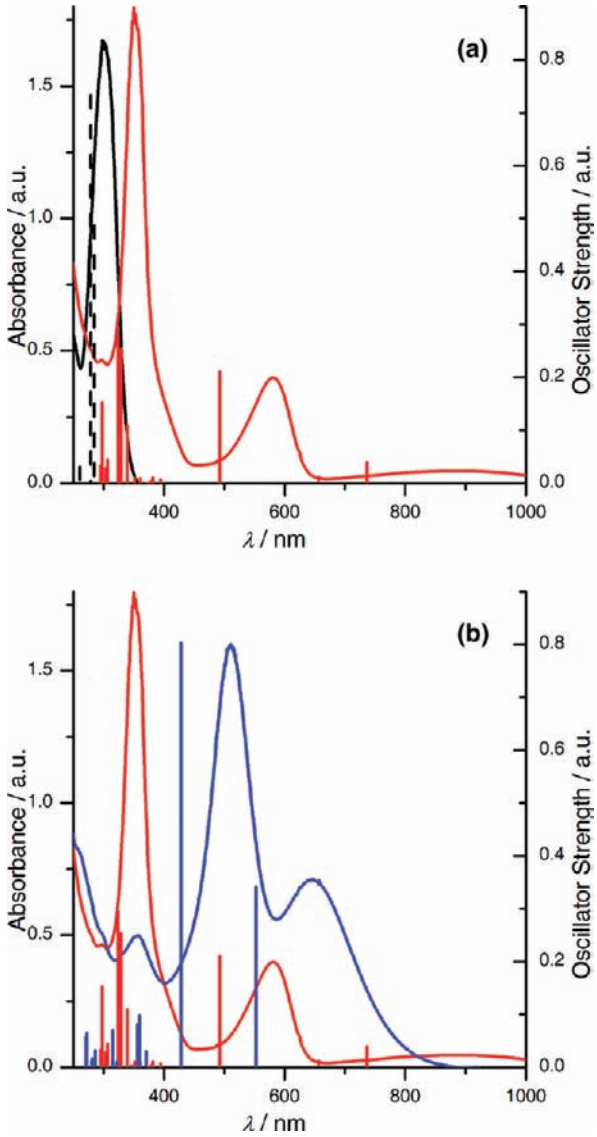

Figure 7. UV−vis−NIR spectroelectrochemistry of Me-**TP**. Superimposed experimental plots (black, $[\text{Me-}\mathbf{TP}]^{+}$ native; red, $[\text{Me-}\mathbf{TP}]^{0}$ singly reduced; blue, $[\text{Me-}\mathbf{TP}]^{-}$ doubly reduced) and corresponding calculated electronic transitions: pyramidal (solid vertical lines) and axial (dashed vertical lines). (a) $[\text{Me-}\mathbf{TP}]^{+}$ and $[\text{Me-}\mathbf{TP}]^{0}$. (b) $[\text{Me-}\mathbf{TP}]^{0}$ and $[\text{Me-}\mathbf{TP}]^{-}$. Note that no energy minimum was found for *reduced* axial forms (see Table S4).

electronic transitions was found to match properly the experimental spectrum of the reduced electrophore in the sole case of the pyramidal doubly reduced species $[\text{qPy-}\mathbf{TP}(\text{pyramid})]^{0}$ (see Figures 8 and S3), also computed to be more stable than the axial one $[\text{qPy-}\mathbf{TP}(\text{axial})]^{0}$ (Table S2).

Experimentally, no isosbestic point is observed during the reduction of $[\text{qPy-}\mathbf{TP}]^{2+}$ to $[\text{qPy-}\mathbf{TP}(\text{pyramid})]^{0}$ (Figure 8 and Supporting Information). This is indicative of a reduction process which is more complex than a mere direct transfer of a couple of electrons. This observation is consistent not only with an intervening interconversion equilibrium of singly reduced electromers (eq 5 in section 3.2), but also with only a moderate propensity of these latter ($[\text{qPy-}\mathbf{TP}]^{+}$) to disproportionate. These findings further support the assumption that the *N*-pyramidalization is correlated with the two-electron reduction process, moreover involving intermediate electromeric species.

dx.doi.org/10.1021/ja210024y | *J. Am. Chem.Soc.* 2012, 134, 2691−2705

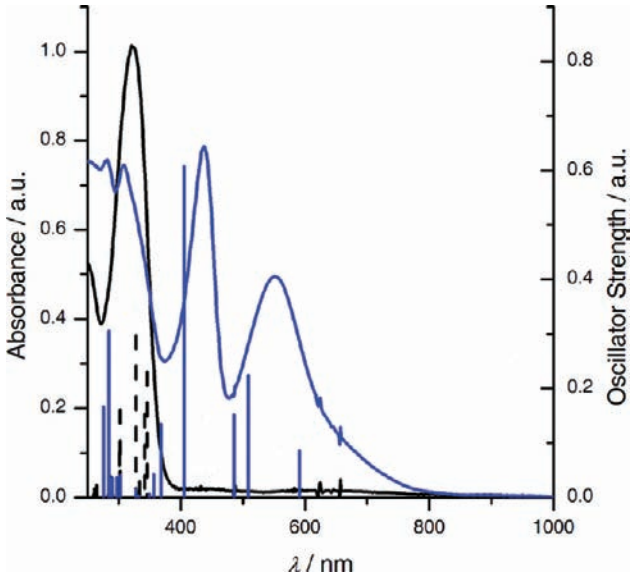

Figure 8. UV−vis−NIR spectroelectrochemistry of qPy-**TP**. Superimposed experimental plots (black, $[qPy\text{-}\mathbf{TP}]^{2+}$ native; blue, $[qPy\text{-}\mathbf{TP}]^{0}$ doubly reduced) and corresponding calculated electronic transitions: pyramidal (solid vertical lines) and axial (dashed vertical lines). Calculated electronic features of the $[qPy\text{-}\mathbf{TP}]^{+}$ singly reduced form (both axial and pyramidal) are given in Supporting Information.

Last, it is worth noting that the overall shape of the electronic spectrum of $[qPy\text{-}\mathbf{TP}]^{0}$ is closely akin to that of $[Me\text{-}\mathbf{TP}]^{-}$, indicating that the chromophoric entities are roughly the same in both cases. Assuming that there is no σ or π dimerization (pimerization),[40] both the Me-**TP** and qPy-**TP** species should lead, after two-electron reduction, to *N*-pyramidalized carbanions.

A detailed analysis of the MOs involved in the electronic transitions computed for the pyramidal doubly reduced species of both Me-**TP** and qPy-**TP** further confirms this picture. Both species have their HOMO localized on the pyridinium core and their strongest electronic transitions are all of the HOMO−(LUMO+*n*) type (Tables S5 and S6). The spectral features in the visible−NIR region (λ > 400 nm) are the signature of the distorted pyridinium core. Interestingly, in the case of doubly reduced qPy-**TP**, the structural decoupling of the qPy aryl group due to *N*-pyramidalization makes its contribution to the HOMO practically negligible. Nonetheless, qPy mainly contributes to the LUMO and (LUMO+2) orbitals of the doubly reduced electrophore and participates in its chromophoric activity (Supporting Information).

In the case of qLu-**TP** (Figure 9), it was possible to study the electrochromic properties of the one-electron ($[qLu\text{-}\mathbf{TP}]^{+}$) and two-electron ($[qLu\text{-}\mathbf{TP}]^{0}$) reduced species separately, in their pure form. For $[qLu\text{-}\mathbf{TP}]^{+}$ (Figure 9a), the more diagnostic spectral domain is the NIR: the experimental plot agrees well with the two electronic transitions computed at 831 and 1370 nm[38] for $[qLu\text{-}\mathbf{TP}(axial)]^{+}$, but does not match at all the set calculated for $[qLu\text{-}\mathbf{TP}(pyramid)]^{+}$, whose computed lowest-energy transition lies at 616 nm (with a very weak oscillator strength, *f*, of about 0.021; Table S7). The structure in solution of the singly reduced qLu-**TP** electrophore is therefore unambiguously *axial*, in agreement with its computed greater stability (Table S2). Furthermore, for the SOMO−LUMO transition at 1370 nm,[38] it is interesting to note that the SOMO displays an important contribution centered on the lutidylium

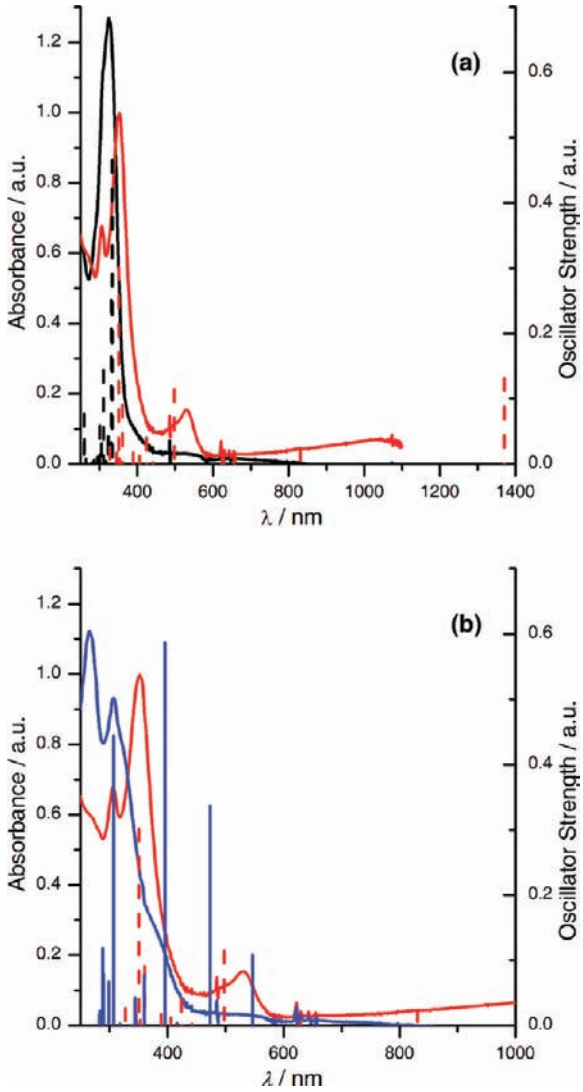

Figure 9. UV−vis−NIR spectroelectrochemistry of qLu-**TP**. Superimposed experimental plots (black, $[qLu\text{-}\mathbf{TP}]^{2+}$ native; red, $[qLu\text{-}\mathbf{TP}]^{+}$ singly reduced; blue, $[qLu\text{-}\mathbf{TP}]^{0}$ doubly reduced) and corresponding calculated electronic transitions: pyramidal (solid vertical lines) and axial (dashed vertical lines). (a) $[qLu\text{-}\mathbf{TP}]^{2+}$ and $[qLu\text{-}\mathbf{TP}]^{+}$.[38] (b) $[qLu\text{-}\mathbf{TP}]^{+}$ and $[qLu\text{-}\mathbf{TP}]^{0}$.

substituent, which is actually made possible by the axial nature of the electromer ($[qLu\text{-}\mathbf{TP}(axial)]^{+}$). For $[qLu\text{-}\mathbf{TP}]^{0}$, both the pyramidal and the axial structures correspond to minima on the PES (Table S2).[30] However, comparison of the experimental spectrum (Figure 9b) with the shapes of the sets of electronic transitions computed for $[qLu\text{-}\mathbf{TP}(axial)]^{0}$ and $[qLu\text{-}\mathbf{TP}(pyramid)]^{0}$, shows that the pyramidal electromer is the more likely in solution. Indeed, the strongest electronic transition of $[qLu\text{-}\mathbf{TP}(axial)]^{0}$ is predicted at around 800 nm (at 793 nm with f = 0.12 and at 762 nm with f = 0.42) along with a second intense transition at 514 nm (f = 0.37), whereas experimentally the red-edge absorption is situated at around 600 nm, with all the main significant bands positioned in the UV−near-visible region (200−450 nm). On the other hand, the dominant electronic transition computed for $[qLu\text{-}\mathbf{TP}(pyramid)]^{0}$ (Table S7) is at ca. 400 nm (395 nm, f = 0.58), with three weaker satellite transitions calculated at 307 (f = 0.44), 473 (f = 0.34), and 546 nm (f = 0.10). It follows that the spectrum recorded at the end of the

dx.doi.org/10.1021/ja210024y | J. Am. Chem.Soc. 2012, 134, 2691−2705

second reduction is that of the pyramidal electromer, [qLu-**TP**(pyramid)]^0, thereby further substantiating the unexpected finding that the energy barrier related to the steric hindrance of the lutidylium group can be overcome by the gain of energy associated with the hybridization change. This overall picture is consistent with the computed relative stabilities: the axial electromer is indeed the more stable for the singly reduced form ([qLu-**TP**(axial)]$^+$), whereas the pyramidal electromer ([qLu-**TP**(pyramid)]^0) is the more stable bireduced species, even though computed to be somewhat less stable[30] and almost isoenergetic with the axial one ([qLu-**TP**(axial)]^0), in line with the electrochemical findings of section 3.2 (i.e., irreversibility of the second reduction). It is also interesting to note that, analogous to the doubly reduced Me-**TP** and qPy-**TP** pyramidal species, in the case of the most stable [qLu-**TP**(pyramid)]^0 electromer the HOMO is essentially localized on the pyridinium core, and the dominant transitions observed are all of the HOMO-to-(LUMO+*n*) type (Supporting Information).

3.4. Integrated Overall Picture: Toward Steric Switching of Potential Compression/Inversion. To complete the assessment of the observed potential compression (**TP** series) or inversion (**XP** series), it is worth considering the possible role of solvation that may be significant.[8,41] Solvent stabilization varies roughly as the square of the charge, according to the Born treatment.[8] Therefore, from the viewpoint of electrostatics, one should distinguish between electrophores whose charge decreases steadily upon reduction, as for dicationic *head-to-tail*-bipyridinium species (Ar = qPy and qLu), going from +2 for the native state to zero for the fully reduced form, and the monocationic electrophores whose charge goes from +1 to zero and −1. The solvent used in the present study, MeCN, is an electron-donating solvent that tends to stabilize cations and destabilize anions. Solvent stabilization, therefore, is expected to steadily decrease upon reduction of dicationic native electrophores. Also, neutral singly reduced monopyridinium-based electrophores (i.e., monocationic native EPs) are hardly stabilized by solvation; neither are their monoanionic doubly reduced derivatives as compared to their monocationic native parents. In fact, the same electrochemical behavior, namely single-step two-electron reduction, is observed regardless of the sequence of charge change. This persistence of the phenomenon of potential compression/inversion rules out any determining role of the solvent in the observed electrochemical process. Besides, solvation energy is not of the same order of magnitude as that required for *N*-pyramidalization. Ion-pairing effects are also ruled out by roughly the same reasoning, but also in view of the chemical nature of the electrophores and the counter-anions involved (PF_6^- or BF_4^-), which are poorly nucleophilic.

Now that we have a clear-cut picture of the origin of single-step two-electron reductions, the complete set of computed data can be checked against available experimental data. Graphical representations have been chosen to display the relevance of the synthetic strategy (Chart 1) developed to establish the existence of the *N*-pyramidalization as the key structural rearrangement explaining the potential compression/inversion and to further substantiate it. In Figure 10 are superimposed computational results based on the assumption of *N*-pyramidalization correlated with reduction (Tables S2 and S4) and experimental measurements of reduction potentials, along with the associated number of electrons (Table 1) for the prototypical Ar-**TP** electrophore. Similar graphs for Ar-**XP** and

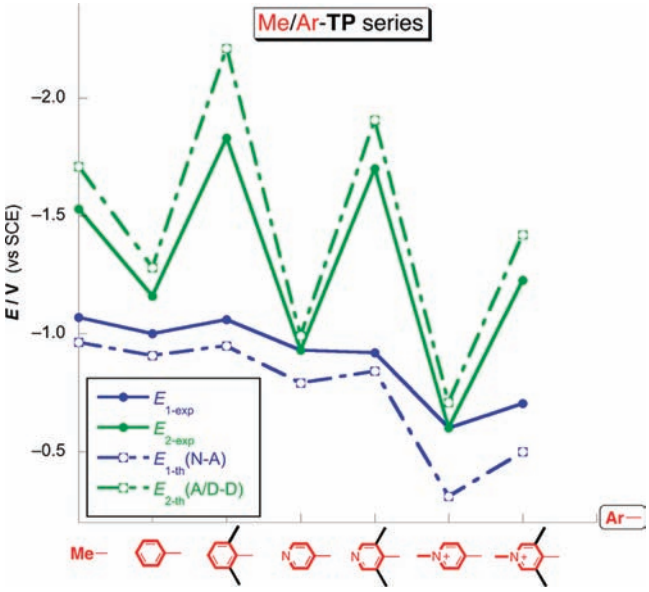

Figure 10. On/off switching of the potential compression for the Ar-**TP** series of electrophores (configurational gating of reduction processes), based on experimental data (E_{exp}; Table 1), calculated data (E_{th}; Tables S2 and S4), and assuming that (1) there is an interconversion equilibrium of electromers when Ar = Ph, Py, and qPy (1st reduction, $E°$(red1)/(N−A); 2nd reduction, $E°$(red2)/(D−D)) and (2) the *N*-pyramidalization is somehow concerted with the second one-electron reduction when Ar = Xy, Lu, and qLu (1st reduction, $E°$(red1)/(N−A); 2nd reduction $E°$(red2)/(A−D)), as proposed in section 3.2. N, A, and D refer to the native (axial), axial, and distorted (pyramidal or bent) forms, respectively (see Supporting Information).

Ar-**DMTP** electrophores are given in Supporting Information (Figures S7 and S8).

The whole idea was to show that by manipulating appropriate structural parameters, it was possible to switch on/off this compression or inversion of potential and thereby to demonstrate the accuracy of our explanation (Figure 1). As shown in Figure 10, there is an obvious agreement between experimental and theoretical results that definitively validates the quality of the modeling as well as the relevance of the working hypotheses. Only a slight discrepancy between experimental and calculated values of standard potential is noted in the case of qPy-**TP**, which is ascribed to self-interaction error.[30,42]

The radical change of electrochemical properties revealed by their switchability also demonstrates that steric strain can produce effects that compare well with those classically obtained by modifying the strength of electron-withdrawing/releasing substituents, referred to as electronic effects. In other words, provided that electrophores undergo compression/inversion of potential as a result of structural rearrangement, steric tuning becomes competitive with electronic tuning of their redox properties. Most importantly, we show here that even the ability of an electrophore to store one or two electrons at a given potential can be controlled and manipulated, which is quite unusual.

3.5. Further Delineation of the Role of the *N*-Pyridinio Group: Insights from Theory. MOs computed for various model electrophores are analyzed in this section in order to get a more precise although qualitative idea of the respective roles of the *N*-pyridinio aryl groups and the pyridinium cores (Figure 1) at the structural or electronic levels.

dx.doi.org/10.1021/ja210024y | *J. Am. Chem.Soc.* 2012, 134, 2691−2705

Comparison of the LUMOs of various electrophores in their axial native forms reveals that the electron exchanged first is attached to the core pyridinium or to the *N*-pyridinio aryl group (Ar) depending on whether the electrophore is monocationic (e.g., Py-**TP**) or dicationic (e.g., qPy-**TP**), as expected[11] (Figure 11). However, in the latter case, it is worth noticing that the $N_{pyridinio}$ atom of the pyridinium core is fully involved in this LUMO. These different characteristics are shared by all electrophores of the same charge.

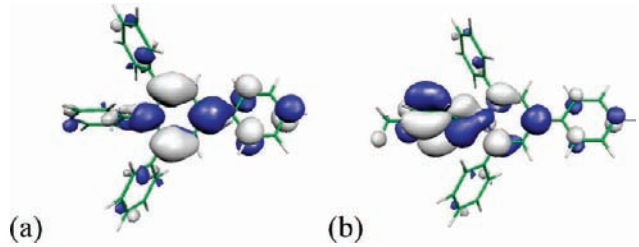

Figure 11. Switching of the site of first reduction upon quaternization. (a) LUMO of Py-**TP** (the pyridinium core is reduced first). (b) LUMO of qPy-**TP** (the pendant pyridylium is reduced first); isocontour = 0.025.

To clarify the status of quaternized aryl groups (qPy or qLu), which are naturally expected to play an electrophoric role, in the sense of "charge/electron holders/carriers", it is interesting to scrutinize the relevant frontier orbitals (LUMO, SOMO, and HOMO) of a representative species, qPy-**TP**, in its different reduction states including electromeric axial and pyramidal forms (Figure 12).

The first striking point is that, in all cases, whether for axial or pyramidal forms including electromers, the LUMO remains essentially located on the pyridylium aryl group. As a consequence, the incoming electron is first attached to this part of the electrophore, including in the second reduction of the pyramidal electromer. Similar conclusions are reached by close analysis of the frontier MOs of lutidylium derivatives (Ar = qLu; Figure S6 in Supporting Information).

The second point concerns the SOMO and HOMO of relevant pyramidal one- and two-electron-reduced electrophores, respectively. These MOs give an indication as to where the electron density is after the first and second reduction.[43] In both cases, electrons are located essentially on the pyridinium core. Thus, one could see these pyridylium or lutidylium aryl groups as a kind of "antenna" for electrons, which are subsequently channeled to the site of the pyridinium core, where they are temporary stored. Note that under the (wrong) assumption that electrophores remain axial upon reduction, incoming electrons are finally stored (SOMO and HOMO) at the site where they were first attached (LUMO); i.e., there is no intramolecular shift of electron density (Figure 12). When the aryl group is virtually redox-inactive (Ar = Ph, Xy) or far less redox-active than the pyridinium core (Ar = Py, Lu), that is, in the case of monocationic electrophores, incoming electrons (of the first and second reductions) are directly attached to the pyridinium core. These findings also hold for other dicationic and monocationic electrophores of the **XP** and **DMTP** types. In other words, if the aryl group of branched EPs is not really involved in the electrophoric properties (i.e., does not carry electron(s)), it may function as an "electron antenna".

In the case of heavily constrained electrophores (Ar-**XP** and Ar-**DMTP** with Ar = Xy, Lu, and qLu), for which no single-step two-electron reduction is observed, the situation can be quite different (see Figure 13). Not only is *N*-pyramidalization hindered, but also the electron-accepting strength of this pyridinium core is weakened by slightly electron-donating electronic effects of β substituents (i.e., Me and canted Ph),[33] as shown by the electrochemical study (Table 1, section 3.2).

As regards steric effects, inspection of doubly reduced species is instructive (Figure 13, top). Thus, given the same lutidyl aryl group (Lu), *N*-pyramidalization is computed for the **XP** electrophore (pyramidalization is driven to completion) whereas the backbone is only bent in the case of the **DMTP** analogue (onset pyramidalization; see also Figure 6). This finding is ascribed to the fact that the methyl substituents at the β positions (R′ in Chart 1) are sterically more demanding than the canted phenyl rings, due to their "ball-shaped" van der Waals volume. These methyl substituents indirectly produce a larger steric strain in the whole environment of the pyridinium platform, leaving no room for a large structural rearrangement like *N*-pyramidalization. The second significant observation is that on going from Lu to qLu as the aryl group for the same **XP** electrophore, the distortion changes from pyramidal to only bent. This tendency is explained by the larger electron-withdrawing ability of the qLu group, which promotes a certain degree of intramolecular intersite electronic delocalization that is expressed due to the synergistic assistance of the overall steric crowding. Accordingly, qLu takes part in the electrophoric function, unlike Lu, as revealed by the spatial extension of the HOMO that affects the qLu moiety. The same delocalization effect is evidenced for the **DMTP** analogues and is revealed by

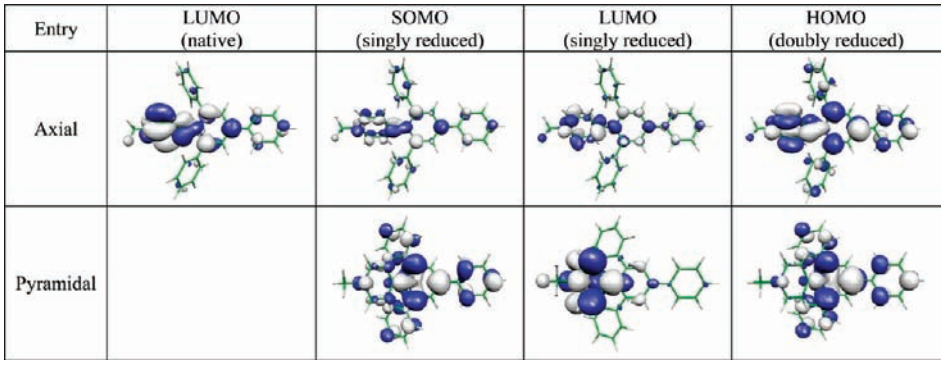

Figure 12. Relevant frontier MOs of qPy-**TP** in axial and pyramidal geometries (isocontour = 0.025). For the shape of the lone pair of the pyramidalized nitrogen atom in doubly reduced qPy-**TP**, see Figure S5 in Supporting Information.

dx.doi.org/10.1021/ja210024y | *J. Am. Chem.Soc.* 2012, 134, 2691−2705

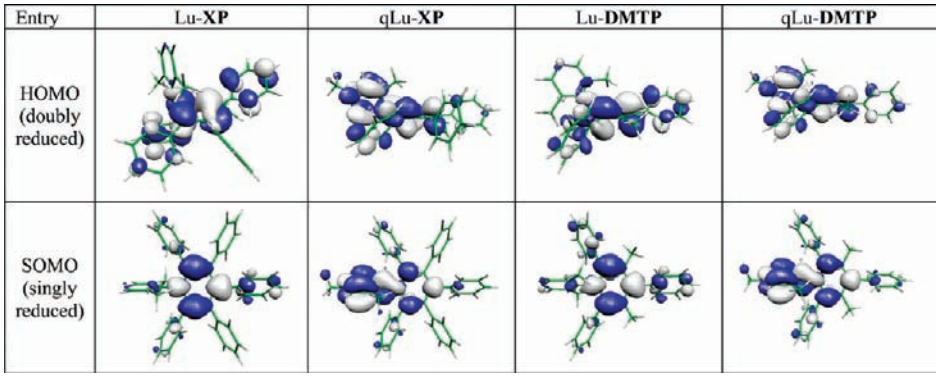

Figure 13. HOMOs (top) and SOMOs (bottom) of electrophores Lu/qLu-**XP** and Lu/qLu-**DMTP** in their doubly and singly reduced forms, respectively (isocontour = 0.025).

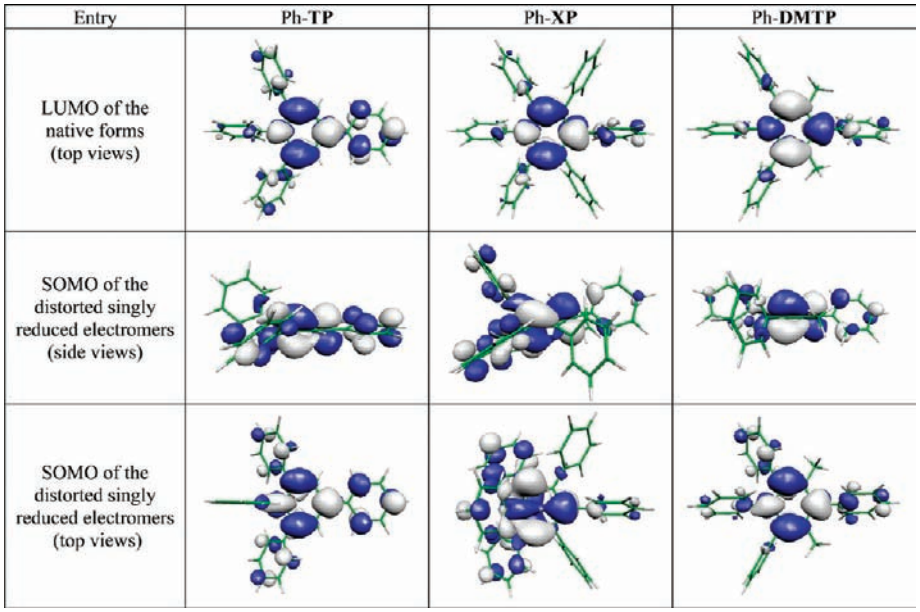

Figure 14. LUMOs and SOMOs of electrophores Ph-**TP**, Ph-**XP**, and Ph-**DMTP** in their native axial and distorted singly reduced forms (isocontour = 0.025).

the less pronounced bending of the electrophore when Ar = qLu than when Ar = Lu (Figure 13 top).

The electrophoric role of the bulky quaternized aryl groups (qLu) within these constrained electrophores is conserved in both the axial one-electron-reduced and bent two-electron-reduced structures (e.g., qLu-**XP** and qLu-**DMTP**; Figure 13). It is worth recalling that this electrophoric contribution vanishes for all three types of electrophores (i.e., **TP**, **XP**, and **DMTP**) with a sterically less demanding aryl group like qPy, as a consequence of the intervening pyramidalization (Figure 12 and Supporting Information), as previously shown.

On the basis of the foregoing, the borderline behavior of Ph-**TP**, Ph-**XP**, and Ph-**DMTP** in their one-electron-reduced states, in which the phenyl group is considered as redox-inactive and almost neutral as regards electronic effects, can now be rationalized. Compared to pyridyl and pyridylium analogues (Ar = Py and qPy), which all adopt a pyramidal structure in one of their singly reduced electromeric forms, not all the phenyl derivatives follow this trend. The geometry of distorted electromers is bent, pyramidal and loosely bent (almost axial) for Ph-**TP**, Ph-**XP**, and Ph-**DMTP**, respectively (Figure 14). Other things being equal (in particular intramolecular steric strain), the main difference between Ph and Py/qPy derivatives stems from the electron-withdrawing ability of the latter aryl groups.

This observation suggests the following explanation for the onset pyramidalizations (bent structures): not enough electron density is withdrawn (shifted) toward the $N_{pyridinio}$ atom to drive its hybridization change to completion when Ar = Ph. The spin density remains on the C4 position of the reduced pyridinium core, as is usually the case.[4g,44] Clearly, in the basic case of Ph-**TP**, the steric strain is moderate and is normally easily overcome. In the borderline case of Ph-**XP**, the role of the steric strain on *N*-pyramidalization is revealed by the complete hybridization change. This is assisted *directly* by the phenyls on either side of the $N_{pyridinio}$ atom (as was demonstrated for Me-**PP** and Ph-**PP** models; see note S1 in Supporting Information) and *indirectly* by the β substituents on the pyridinium core (R′ = Ph and Me; Chart 1). In the case of Ph-**DMTP**, the further increase in steric strain overcomes the weak driving force for the hybridization change postulated in the case of Ar = Ph. There is therefore little pyramidalization, and only slight bending is observed (Figure 14). In all three cases, however, the doubly reduced electrophore is pyramidalized, giving

dx.doi.org/10.1021/ja210024y | *J. Am. Chem.Soc.* 2012, 134, 2691−2705

rise to a compression of potential for Ph-**TP** with two closely lying one-electron reductions (Figure 2),[9] an inversion of potential with a single-step two-electron reduction for Ph-**XP**,[9] and a complex electrochemical−chemical−electrochemical (ECE) behavior[31] for the particular Ph-**DMTP**.

To summarize, the following picture emerges from close analysis of the active MOs and related optimized geometries of model electrophores in their various reduction states:

- It is possible to establish a direct relationship between the electrophoric character (electron carrier/holder) of a group/component and its involvement in a mesomeric effect, which is itself conditioned by the type of structure (axial, bent or pyramidal) hosting this group. Typically, as far as branched expanded pyridiniums are concerned, qPy and qLu aryl groups are *potentially* electrophoric, contrary to Ph, Xy, Py, and Lu groups. However, qPy and qLu are *effectively* electrophoric in the case of axial and bent molecular geometries only (i.e., not in pyramidalized structures).
- In the case of electrophores adopting a pyramidal structure (whether there be electromers or single forms), these qPy and qLu groups contribute to the properties of electrophores both by *interfacing* the electron exchange (i.e., "by collecting incoming electrons") and by *shifting* this electron density toward the $N_{pyridinio}$ atom of the core, *like an antenna system*.
- The *increase in spin density on the site of the* $N_{pyridinio}$ *atom is identified as the triggering event for the change of hybridization*, regardless of whether this electron density comes from the "antenna" aryl group (Ar = qPy and qLu) or from the directly reduced pyridinium core itself (when Ar = Xy, Ph, Py, and Lu). In the latter case, slightly electron-withdrawing Py and Lu groups are better at localizing the spin density appropriately than Ph and Xy groups.
- Whether this change of hybridization is indeed easily achieved or not is a matter of a complex balance between possibly conflicting structural and electronic factors. Clearly, the steric crowding of the pyridinium core assists the distortion, i.e. the change of hybridization of its $N_{pyridinio}$ atom.
- The pyramidalization of electrophores in their singly reduced form, whether or not as electromers, is crucial for the observation of a single-step two-electron reduction, as demonstrated by the steric switching of electrochemical properties (Figure 10). This particular distorted substructure is the only one able to handle two electrons easily, that is, to minimize the adverse Coulombic repulsion between these electrons, hence its ability to undergo a second reduction at the same potential as the first one.
- As confirmed by the combined spectroelectrochemical/TD-DFT study, the pyramidalized pyridinium core is the only electrophoric component that is observed subsequent to two-electron reduction of the reference electrophore, qPy-**TP**.

4. CONCLUSION

We have shown that the ability of branched expanded pyridinium to accept (i.e., store) one or two electrons can be sterically gated. Elucidation of the origin of the single-step two-electron reduction, namely a potential compression/inversion involving a dynamic fluxional behavior[32] between redox isomers (electromers), is an important step forward.

From the present combined experimental and theoretical study, the picture we obtain of branched expanded pyridiniums is that of complex electrophores. The aryl group serves not only for its structural hindrance and its electron-withdrawing ability; it can also function as a kind of "electron antenna"[45] that collects electrons (interfacial exchange site), while the pyridinium core plays the role of the very electrophoric unit (electron carrier) that ultimately traps the two electrons. Overall, we introduce here a new functional paradigm: the particularly fortunate association of the electrophoric pyridinium motif with intramolecular steric hindrance about the nitrogen atom that results in the phenomenon of *N*-pyramidalization. We demonstrate that this latter confers upon the thus-modified pyridinium its ability to undergo apparently a two-electron process. The reorganization energy of electromers subsequent to the first one-electron transfer (more than) compensates adverse electrostatic factors, thereby allowing a second one-electron transfer at the same potential, which otherwise would occur at a sizably different potential (as observed when the structural rearrangement is hindered).[46]

Moreover, when the intramolecular balance between steric strain and electronic factors is properly adjusted, the two-electron process becomes reversible.

Insights gained from the above analysis make it possible to derive guidelines for future design of molecular devices meant for multielectron handling, including storage.

Beyond the switchability of electrochemical behavior, other applications of the interplay between redox and structural properties can be considered, for example to produce mechanical work at the molecular level (electromechanical molecular actuators).[20] Of particular interest in the context of the present study is the possibility of harnessing these electrophores that exhibit a large redox-driven structural rearrangement with another functional element such as a photoactuator (e.g., azobenzene) able to photoproduce a steric strain on this electrophore. In doing so, not only the electron storage ability of the modified electrophore could be controlled, but also the triggering of the release or uptake of two electrons, depending on whether the active electrophore is in its reduced or native form (toward smart donors/acceptors of *two* electrons).

Last, the existence of the *N*-pyramidalization induced by reduction and the understanding of the manner by which this configurational change can be monitored are of practical interest for the design of molecular wires made up of pyridinium subunits.[4a−c,47,48]

5. EXPERIMENTAL SECTION

5.1. Syntheses, Characterization and General Experimental Details. Materials, syntheses of the EPs and related ferrocenyl dyads, and full characterizations are provided in Supporting Information.

5.2. Computational Methods. The first reduction potential toward a standard hydrogen electrode (SHE) was computed as

$$E_{1/2}(V) = \frac{(\Delta G_{nat} - \Delta G_{red})}{F} + E_{SHE}$$

F being the Faraday constant (23.06 kcal mol^{-1} V^{-1}) and E_{SHE} being set to 4.44 V. The difference in free energies between the native and reduced forms (Gibbs free energy, ΔG in kcal mol^{-1}) computed under standard conditions (T = 298.15 K and P = 1 atm) were used to evaluate their relative stabilities as previously reported (see for instance ref 49).

dx.doi.org/10.1021/ja210024y | J. Am. Chem.Soc. 2012, 134, 2691−2705

Analogously, the second reduction potential was computed as

$$E_{1/2}(V) = \frac{(\Delta G_{\text{red-1}e^-} - \Delta G_{\text{red-2}e^-})}{F} + E_{\text{SHE}}$$

where $\Delta G_{\text{red-1}e^-}$ and $\Delta G_{\text{red-2}e^-}$ represent the Gibbs free energies of the one- and two-electron-reduced electrophores, respectively.

All free energies were computed at the DFT level using the hybrid exchange-correlation functional PBE0[50] in conjunction with a double-ζ all-electron basis set.[51]

In order to assess the nature of the one- and two-electron-reduced species, additional calculations were performed using a range-separated hybrid functional (CAM-B3LYP[52]) and a larger basis set (the Pople 6-31G(d) basis). The structures of native, singly reduced, and doubly reduced forms of the Me-**TP**, qPy-**TP**, and qLu-**TP** systems were fully optimized at this level of theory, and all stationary points so obtained were characterized as minima by subsequent frequency calculations.

The spectral features (i.e., vertical absorption energies and associated oscillator strengths) of each of these forms were computed at the TD-DFT level using both the CAM-B3LYP and the PBE0 functional in conjunction with the larger (6-31+G(d)) basis set. Data reported in the text and figures refer to TD-DFT calculations performed using the PBE0 functional, since CAM-B3LYP yields qualitatively similar results in slightly poorer agreement with experimental data, as expected. In all cases solvent effects were taken into account using the Polarizable Continuum Model (PCM[53]) as implemented in the Gaussian code,[54] and MeCN was considered as solvent (experimentally used solvent).

All calculations were performed using the Gaussian program (Gaussian 09).[55]

5.3. Electrochemical Measurements. Electrochemical experiments were carried out with a conventional three-electrode cell and a PC-controlled potentiostat/galvanostat (Biologic VSP or Princeton Applied Research Inc. model 263A). The working electrode was a platinum electrode from Radiometer-Tacussel (area, 0.0314 cm^2; diameter, 2.0 mm) mounted in Teflon. Before each experiment, it was carefully polished with 3 and 0.3 μm alumina pastes followed by extensive rinsing with ultrapure Milli-Q water. Platinum wire was used as the counter-electrode and a saturated calomel electrode (SCE) as the reference. Electrolytic solutions, MeCN (Aldrich, anhydrous, 99.8%) containing 0.1 M tetrabutylammonium hexafluorophosphate ($TBAPF_6$, Aldrich, +99%) as supporting electrolyte, were routinely deoxygenated by argon bubbling. The electrochemical properties were determined using a monomer concentration of ca. 5 mM. All potential values are given versus SCE. The reported numerical values (Table 1) were corrected by using a dissolved Fc^+/Fc couple as an internal reference and by setting $E_{1/2}$ (Fc^+/Fc) equal to +0.380 V vs SCE in MeCN.[56] CV experiments were conducted at a scan rate of 0.1 V s^{-1} (except where specified in the text). RDE voltammetry experiments were conducted at a scan rate of 0.05 V s^{-1} (except where specified in the text) by rotating the disk electrode at 2000 rpm (Controvit device from Radiometer-Tacussel, France). Square-wave voltammetry experiments were performed with potential sweep rate of 100 mV s^{-1} (pulse height, 25 mV; step height, 10 mV; frequency, 50 Hz).

5.4. UV−Vis−NIR Spectroelectrochemical Measurements. The prototype of the spectroelectrochemical optically transparent thin-layer electrode (OTTLE) cell was developed in the J. Heyrovský Institute, and its construction was fully described by Krejčík et al.[57] The current modified version of the cell is commercially available from the Department of Chemistry, University of Reading, UK.[58] The steel body of the cell uses the demountable Specac cell, model Omni-Cell GS01800 (Specac Ltd., Orpington, UK).[59] Two CaF_2 windows form a thin-layer cell, the thickness of which is given by a 0.19 mm polyethylene spacer. The working and counter electrodes consist of two platinum minigrids (wire diameter, 0.075 mm; 80 mesh woven) placed 8 mm apart. The reference electrode is a silver wire coated with a layer of AgCl, placed 2 mm from the working electrode. The electrical connections to a potentiostat are made through Pt wires melt-sealed in the plastic spacer mentioned above. The light path is masked so that the beam passes through the center of the working electrode. The inlet and outlet openings allow filling the cell with degassed samples under anaerobic conditions. Cyclic voltammograms obtained concurrently with the UV−vis−NIR spectra were recorded using a potentiostat/galvanostat Autolab 101 (Metrohm Autolab, Netherlands) at scan rates of 10 mV s^{-1}, while the spectra were sampled every 2 s using a diode-array UV−vis−NIR spectrometer (Agilent, model 8453). $TBAPF_6$, (+99%) supporting electrolyte and MeCN solvent (anhydrous, 99.8%) were supplied by Sigma-Aldrich and dried before use.

■ ASSOCIATED CONTENT

Supporting Information

Complete refs 1 and 55; computational results including optimized structures, calculated standard potentials, and stabilities of reduced EPs along with their related electronic properties (TD-DFT) and structures (involved frontier MOs); full data related to spectroelectrochemical studies; selected cyclic and RDE voltammograms; preliminary ESR data; experimental details for the synthesis and characterization of new compounds and precursors including ^1H NMR (500 MHz) and ^{13}C NMR (126 MHz) spectra as well as ESI mass spectra. Cartesian coordinates of optimized structures and corresponding total energies. This material is available free of charge via the Internet at http://pubs.acs.org.

■ AUTHOR INFORMATION

Corresponding Author

philippe.laine@univ-paris-diderot.fr; ilaria-ciofini@chimie-paristech.fr; hromadom@jh-inst.cas.cz

■ ACKNOWLEDGMENTS

Prof. Sebastiano Campagna and his group, Dr. Sophie Griveau, Prof. Cyrille Costentin, and Dr. John Lomas, are acknowledged for stimulating discussions. J.F., V.M., G.D., C.A., I.C., and P.P.L. are grateful to the French National Agency for Research (NEXUS project ANR-07-BLAN-0277 and SWITCH project ANR-2010-BLAN-712) for financial support.

■ REFERENCES

(1) Adams, D. A.; et al. *J. Phys. Chem. B* **2003**, *107*, 6668.

(2) (a) Joachim, C.; Ratner, M. A. *Proc. Natl. Acad. Sci. U.S.A.* **2005**, *102*, 8801. (b) Joachim, C.; Gimzewski, J. K.; Aviram, A. *Nature* **2000**, *408*, 541.

(3) For selected recent reviews, see: (a) Gust, D.; Moore, T. A.; Moore, A. L. *Acc. Chem. Res.* **2009**, *42*, 1890. (b) Magnuson, A.; Anderlund, M.; Johansson, O.; Lindblad, P.; Lomoth, R.; Polivka, T.; Ott, S.; Stensjö, K.; Styring, S.; Sundström, V; Hammarström, L. *Acc. Chem. Res.* **2009**, *42*, 1899. (c) Tinker, L. L.; McDaniel, N. D.; Bernhard, S. *J. Mater. Chem.* **2009**, *19*, 3328. (d) Balzani, V.; Credi, A.; Venturi, M. *ChemSusChem* **2008**, *1*, 26. (e) Eisenberg, R.; Gray, H. B. *Inorg. Chem.* **2008**, *47*, 1697. (f) Benniston, A. C.; Harriman, A. *Mater. Today* **2008**, *11*, 26. (g) Huyhn, M. H. V.; Meyer, T. J. *Chem. Rev.* **2007**, *107*, 5004. (h) Lewis, N. S.; Nocera, D. G. *Proc. Natl. Acad. Sci. U.S.A.* **2006**, *103*, 15729. (i) McEvoy, J. P.; Brudvig, G. W. *Chem. Rev.* **2006**, *106*, 4455. (j) Konduri, R.; Ye, H.; MacDonnell, F. M.; Serroni, S.; Campagna, S.; Rajeshwar, K. *Angew. Chem., Int. Ed.* **2002**, *41*, 3185.

(4) For selected examples related to the (multielectron) reduction of so-called "(conjugation-)extended viologens" (Takahashi, K.; Nihira, T.; Akiyama, K.; Ikegami, Y.; Fukuyo, E. *J. Chem. Soc., Chem. Commun.* **1992**, 620.), see: (a) Kolivoska, V.; Gál, M.; Pospísil, L.; Valásek, M.; Hromadová, M. *Phys. Chem. Chem. Phys.* **2011**, *13*, 11422. (b) Pospísil, L.; Hromadová, M.; Fanelli, N.; Valásek, M.; Kolivoska, V.; Gál, M. *Phys. Chem. Chem. Phys.* **2011**, *13*, 4365. (c) Pospísil, L.; Hromadová, M.; Gál, M.; Valásek, M.; Fanelli, N.; Kolivoska, V. *Collect. Czech. Chem. Commun.* **2009**, *74*, 1559. (d) Casado, J.; Patchkovskii, S.; Zgierski, M. Z.; Hermosilla, L.; Sieiro, C.; Moreno Oliva, M.;

Lopez Navarrete, J. T. *Angew. Chem., Int. Ed.* **2008**, *47*, 1443. (e) Pospísil, L.; Fiedler, J.; Hromadová, M.; Gál, M.; Valásek, M.; Pecka, J.; Michl, J. *J. Electrochem. Soc.* **2006**, *153*, E179. (f) Funston, A.; Kirby, J. P.; Miller, J. R.; Pospísil, L.; Fiedler, J.; Hromadová, M.; Gál, M.; Pecka, J.; Valásek, M.; Zawada, Z.; Rempala, P.; Michl, J. *J. Phys. Chem. A* **2005**, *109*, 10862. (g) Porter, W. W.; Vaid, T. P.; Rheingold, A. L. *J. Am. Chem. Soc.* **2005**, *127*, 16559. (h) Porter, W. W.; Vaid, T. P. *J. Org. Chem.* **2005**, *70*, 5028.

(5) For selected work dealing with the multielectron reduction of fullerenes, see: (a) Diener, M. D.; Alford, J. M. *Nature* **1998**, *393*, 668. (b) Weaver, M. J.; Gao, X. *J. Phys. Chem.* **1993**, *97*, 332. (c) Yang, Y.; Arias, F.; Echegoyen, L.; Chibante, L. P. F; Flanagan, S.; Robertson, A.; Wilson, L. J. *J. Am. Chem. Soc.* **1995**, *117*, 7801. (d) Xie, Q.; Pérez-Cordero, E.; Echegoyen, L. *J. Am. Chem. Soc.* **1992**, *114*, 3978.

(6) For selected examples concerning oxidizable electrophores (i.e., potentially multielectron donors), that is, star-shaped semirigid and coupled multicenter electrophores, see: (a) Diallo, A. K.; Absalon, C.; Ruiz, J.; Astruc, D. *J. Am. Chem. Soc.* **2011**, *133*, 629. (b) Lambert, C. *Angew. Chem., Int. Ed.* **2005**, *44*, 7337 and references therein.

(7) Han, Z.; Vaid, T. P.; Rheingold, A. L. *J. Org. Chem.* **2008**, *73*, 445.

(8) (a) Evans, D. H. *Chem. Rev.* **2008**, *108*, 2113 and references therein. (b) Evans, D. H.; Hu, K. *J. Chem. Soc., Faraday Trans.* **1996**, *92*, 3983.

(9) Fortage, J.; Tuyèras, F.; Ochsenbein, P.; Puntoriero, F.; Nastasi, F.; Campagna, S.; Griveau, S.; Bedioui, F.; Ciofini, I.; Lainé, P. P. *Chem.—Eur. J.* **2010**, *16*, 11047.

(10) Peltier, C.; Adamo, C.; Lainé, P. P.; Campagna, S.; Puntoriero, F.; Ciofini, I. *J. Phys. Chem. A* **2010**, *114*, 8434.

(11) Fortage, J.; Peltier, C.; Nastasi, F.; Puntoriero, F.; Tuyèras, F.; Griveau, S.; Bedioui, F.; Adamo, C.; Ciofini, I.; Campagna, S.; Lainé, P. P. *J. Am. Chem. Soc.* **2010**, *132*, 16700.

(12) Prototypical complex for a single-electron storage: (a) Astruc, D.; Hamon, J.-R.; Althoff, G.; Román, E.; Batail, P.; Michaud, P.; Mariot, J.-P.; Varret, F.; Cozak, D. *J. Am. Chem. Soc.* **1979**, *101*, 5445. (b) Hamon, J.-R.; Astruc, D.; Michaud, P. *J. Am. Chem. Soc.* **1981**, *103*, 758.

(13) For strategies involving purely organic molecules for two-electron storage, referred to as "super electron donors" (SEDs), see for instance ref 4g and the following: (a) Murphy, J. A.; Garnier, J.; Park, S. R.; Schoenebeck, F.; Zhou, S.-Z.; Turner, A. T. *Org. Lett.* **2008**, *10*, 1227. (b) Murphy, J. A.; Zhou, S.-Z.; Thomson, D. W.; Schoenebeck, F.; Mahesh, M.; Park, S. R.; Tuttle, T.; Berlouis, L. E. A. *Angew. Chem., Int. Ed.* **2007**, *46*, 5178. (c) Richardson, R. D.; Wirth, T. *Chem. Unserer Z.* **2008**, *42*, 190.

(14) For strategies relying on C−C bond forming/breaking, but involving inorganic including organometallic (supra)molecular compounds, also for two-electron storage, see: (a) Venkatesan, K.; Blacque, O.; Fox, T.; Alfonso, M.; Schmalle, H. W.; Berke, H. *Organometallics* **2004**, *23*, 1183. (b) Camp, C.; Mougel, V.; Horeglad, P.; Pécaut, J.; Mazzanti, M. *J. Am. Chem. Soc.* **2010**, *132*, 17374. (c) Floriani, C.; Solari, E.; Franceschi, F.; Scopelliti, R.; Belanzoni, P.; Rosi, M. *Chem.—Eur. J.* **2001**, *7*, 3052. (d) Franceschi, F.; Solari, E.; Scopelliti, R.; Floriani, C. *Angew. Chem., Int. Ed.* **2000**, *39*, 1685. (e) Rosi, M.; Sgamellotti, A.; Franceschi, F.; Floriani, C. *Chem.—Eur. J.* **1999**, *5*, 2914. (f) Franceschi, F.; Solari, E.; Floriani, C.; Rosi, M.; Chiesi-Villa, A.; Rizzoli, C. *Chem.—Eur. J.* **1999**, *5*, 708.

(15) For selected examples of alternative strategies that rely on nanoscale architectures like macrocycles or dendrimers decorated with redox-active components, which could function as molecular batteries, see: (a) Mayor, M.; Lehn, J.-M. *J. Am. Chem. Soc.* **1999**, *121*, 11231. (b) Astruc, D. *New J. Chem.* **2011**, *35*, 764. and references therein. (c) Ronconi, C. M.; Stoddart, J. F.; Balzani, V.; Baroncini, M.; Ceroni, P.; Giansante, C.; Venturi, M. *Chem.—Eur. J.* **2008**, *14*, 8365.

(16) Selected recent references: (a) Meylemans, H. A.; Damrauer, N. H. *Inorg. Chem.* **2009**, *48*, 11161. (b) Hanss, D.; Wenger, O. S. *Eur. J. Inorg. Chem.* **2009**, 3778. (c) Indelli, M. T.; Chiorboli, C.; Flamigni, L.; De Cola, L.; Scandola, F. *Inorg. Chem.* **2007**, *46*, 5630. (d) Benniston, A. C.; Harriman, A.; Li, P.; Patel, P. V.; Sams, C. A. *J. Org. Chem.* **2006**, *71*, 3481. (e) Benniston, A. C.; Harriman, A. *Chem. Soc. Rev.* **2006**, *35*, 169.

(17) (a) Lainé, P.; Bedioui, F.; Ochsenbein, P.; Marvaud, V.; Bonin, M.; Amouyal, E. *J. Am. Chem. Soc.* **2002**, *124*, 1364. (b) Lainé, P.; Bedioui, F.; Amouyal, E.; Albin, V.; Berruyer−Penaud, F. *Chem.—Eur. J.* **2002**, *8*, 3162. (c) Lainé, P.; Amouyal, E. *Chem. Commun.* **1999**, 935.

(18) (a) Lainé, P. P.; Campagna, S.; Loiseau, F. *Coord. Chem. Rev.* **2008**, *252*, 2552. (b) Lainé, P. P.; Bedioui, F.; Loiseau, F.; Chiorboli, C.; Campagna, S. *J. Am. Chem. Soc.* **2006**, *128*, 7510. (c) Lainé, P. P.; Loiseau, F.; Campagna, S.; Ciofini, I.; Adamo, C. *Inorg. Chem.* **2006**, *45*, 5538. (d) Lainé, P. P.; Ciofini, I.; Ochsenbein, P.; Amouyal, E.; Adamo, C.; Bedioui, F. *Chem.—Eur. J.* **2005**, *11*, 3711. (e) Ciofini, I.; Lainé, P. P.; Bedioui, F.; Adamo, C. *J. Am. Chem. Soc.* **2004**, *126*, 10763.

(19) (a) Benniston, A. C.; Harriman, A.; Li, P.; Rostron, J. P.; Harrington, R. W.; Clegg, W. *Chem.—Eur. J.* **2007**, *13*, 7838. (b) Beer, P. D.; Chen, Z.; Grieve, A.; Haggitt, J. *J. Chem. Soc., Chem. Commun.* **1994**, 2413. (c) Kodaka, M.; Kubota, Y. *J. Chem. Soc., Perkin Trans. 2* **1999**, 891. (d) Willner, I.; Ayalon, A.; Rabinovitz, M. *New J. Chem.* **1990**, *14*, 685. (e) Chen, P.; Curry, M.; Meyer, T. J. *Inorg. Chem.* **1989**, *28*, 2271. (f) Wardman, P. *J. Phys. Chem. Ref. Data* **1989**, *18*, 1637. (g) Thummel, R. P.; Lefoulon, F.; Chirayil, S.; Goulle, V. *J. Org. Chem.* **1988**, *53*, 4745. (h) Hünig, S.; Berneth, H. *Top. Curr. Chem.* **1980**, *92*, 1.

(20) The same trends are also often observed for electrophores that function as electron donors (oxidation regime). Examples are mainly found in the field of electromechanical actuators, even though the interplay between structural and redox properties is envisaged from the reverse standpoint of the above-mentioned one. The tuning of the structure is the mechanical output whereas the electrochemistry is the input. Owing to the nature of the electroactive components involved (e.g., oligothienyl or analogues), the HOMO is in this case primarily impacted and thus, oxidation processes. (a) Marsella, M. J.; Reid, R. J.; Estassi, S.; Wang, L.-S. *J. Am. Chem. Soc.* **2002**, *124*, 12507. (b) Jousselme, B.; Blanchard, P.; Gallego-Planas, N.; Delaunay, J.; Allain, M.; Richomme, P.; Levillain, E.; Roncali, J. *J. Am. Chem. Soc.* **2003**, *125*, 2888. (c) Jousselme, B.; Blanchard, P.; Levillain, E.; Delaunay, J.; Allain, M.; Richomme, P.; Rondeau, D.; Gallego-Planas, N.; Roncali, J. *J. Am. Chem. Soc.* **2003**, *125*, 1363. (d) Jousselme, B.; Blanchard, P.; Gallego-Planas, N.; Levillain, E.; Delaunay, J.; Allain, M.; Richomme, P.; Roncali, J. *Chem.—Eur. J.* **2003**, *9*, 5297. (e) Jousselme, B.; Blanchard, P.; Allain, M.; Levillain, E.; Dias, M.; Roncali, J. *J. Phys. Chem. A* **2006**, *110*, 3488.

(21) For one such rare example, but dealing with the steric control of the electron-donating ability of a molecule (oxidation regime), see: Bellec, N.; Boubekeur, K.; Carlier, R.; Hapiot, P.; Lorcy, D.; Tallec, A. *J. Phys. Chem. A* **2000**, *104*, 9750.

(22) Bistable electrophores typically made up of a bridging photochromic switchable unit and two pyridinium termini, for instance, are beyond the scope of the present work. Indeed, the energy change of redox-active MOs not only originates from structural modifications but also largely stems from alterations in the electronic structure of the photochromic linker; see: (a) Gilat, S. L.; Kawai, S. H.; Lehn, J.-M. *Chem.—Eur. J.* **1995**, *1*, 275. (b) Gilat, S. L.; Kawai, S. H.; Lehn, J.-M. *J. Chem. Soc., Chem. Commun.* **1993**, 1439.

(23) (a) Bally, T. *Nat. Chem.* **2010**, *2*, 165. (b) Puschmann, F. F.; Harmer, J.; Stein, D.; Rüegger, H.; de Bruin, B.; Grützmacher, H. *Angew. Chem., Int. Ed.* **2010**, *49*, 385.

(24) Bendikov, M.; Wudl, F.; Perepichka, D. F. *Chem. Rev.* **2004**, *104*, 4891.

(25) (a) Hogiu, S.; Dreyer, J.; Pfeiffer, M.; Brzezinka, K.-W.; Werncke, W. *J. Raman Spectrosc.* **2000**, *31*, 797. (b) Catalan, J.; Garcia de Paz, J. L.; Reichardt, C. *J. Phys. Chem. A* **2010**, *114*, 6226.

(26) A similar strategy based on chemical substitution was, for instance, applied by Hapiot, Lorcy and co-workers to investigate the potential inversion observed in vinylogous tetrathiafulvalene derivatives: see ref 21.

(27) Amongst the 19 model electrophores and 13 ferrocenyl-based dyads show in Chart 1, 14 electrophores and 9 dyads are new. These were synthesized for the present study, with the exception of (q)Lu-**XP** along with the associated ferrocenyl dyad, which could not be

obtained (Supporting Information). The other following compounds are described in previous papers: Me-**TP** and its related dyad,[11] Ph-**TP**[9,17,18] and its related dyad,[9] Ph-**XP** and its related dyad,[9] py-**TP** and its related dyad,[11] as well as qPy-**TP**.[11]

(28) Synthesized ferrocenyl-derivatized electrophores, referred to as dyads, actually show two types of connection scheme: linkage of the two components via the *N*-pyridinio phenyl group (cases of Ph-**TP** and Ph-**XP**; see ref 9 and Figure 2) or via the phenyl at position 4 of the pyridinium core (all other cases; Chart 1). Electrochemical behaviors are not sensitive to this topological difference and allow direct comparison of the various dyads, at least for RDE experiments.

(29) The covalent linking within these dyads allowed to avoid bias inherent in different diffusion coefficients when studying bimolecular systems (e.g., electrophore + Fc).

(30) The slight discrepancy noted in the case of Ar = qPy is ascribed to self-interaction error; refer to discussion in Supporting Information that also deals with the associated case of qLu-**TP**.

(31) From CV and RDE experiments performed on the ferrocenyl dyad related to Ph-**DMTP**, the number of exchange electrons involved in the reduction process is 1.3 instead of 2, as expected from calculations (see Supporting Information). This discrepancy does not call into question the relevance of our present demonstration. In fact, dynamic fluxionality and distortion are key features of these EP electrophores, and it is recognized that the time scale of several elementary processes involved in the complex ECE process of potential compression may lead to a situation where the number of electrons involved is between 1 and 2. For the in-depth study of a molecule behaving in such an unusual manner, see ref 32 and references therein.

(32) Felton, G. A. N.; Petro, B. J.; Glass, R. S.; Lichtenberger, D. L.; Evans, D. H. *J. Am. Chem. Soc.* **2009**, *131*, 11290.

(33) See Note S2 in Supporting Information.

(34) Due to the complexity and flexibility of the systems, the evaluation of the barrier height represents a prohibitive task for the used computational approach.

(35) Savéant, J.-M. *Elements of Molecular and Biomolecular Electrochemistry. An Electrochemical Approach to Electron Transfer Chemistry*; Wiley-Interscience: Hoboken, NJ, 2006.

(36) Macías-Ruvalcaba, N. A.; Evans, D. H. *Chem.—Eur. J.* **2007**, *13*, 4386.

(37) Kraiya, C.; Singh, P.; Evans, D. H. *J. Electroanal. Chem.* **2004**, *563*, 203.

(38) The full absorption spectrum of $[\text{qLu-}\mathbf{TP}]^+$ was recorded between 250 and 1800 nm in a separate spectroelectrochemical experiment, confirming the existence of the electronic transition computed at 1370 nm. A very broad band with λ_{max} at ca. 1250 nm was indeed observed (Supporting Information). Only the onset of this NIR band is shown in Figure 9.

(39) Jacquemin, D.; Perpète, E.; Ciofini, I.; Adamo, C. *Acc. Chem. Res.* **2009**, *42*, 326.

(40) (a) Itoh, M.; Kosower, E. M. *J. Am. Chem. Soc.* **1968**, *90*, 1843. (b) Kimura, K.; Yamada, H.; Tsubomura, H. *J. Chem. Phys.* **1968**, *48*, 440. (c) Macías-Ruvalcaba, N. A.; Evans, D. H. *J. Phys. Chem. C* **2010**, *114*, 1285. (d) Macías-Ruvalcaba, N. A.; Evans, D. H. *J. Phys. Chem. C* **2007**, *111*, 5805. (e) Macías-Ruvalcaba, N. A.; Felton, G. A. N.; Evans, D. H. *J. Phys. Chem. C* **2009**, *113*, 338.

(41) For an illustration of the dramatic effect that solvent can have on the electrochemical behavior of certain electrophores, see: Hapiot, P.; Kispert, L. D.; Konovalov, V. V.; Savéant, J.-M. *J. Am. Chem. Soc.* **2001**, *123*, 6669.

(42) Ciofini, I.; Adamo, C.; Chermette, H. *J. Chem. Phys.* **2005**, *123*, 121102.

(43) In this respect, electron density difference maps are usually the more informative, since they provide a picture of the change in the relaxed electron density. However, in the present case the overall picture obtained from the analysis of these MOs is qualitatively the same.

(44) (a) Kosower, E. M.; Cotter, J. L. *J. Am. Chem. Soc.* **1964**, *86*, 5524. (b) Yasukouchi, K.; Taniguchi, I.; Yamaguchi, H; Shiraishi, M. *J. Electroanal. Chem.* **1979**, *105*, 403. (c) Raghavan, R.; Iwamoto, R. T. *J. Electroanal. Chem.* **1979**, *102*, 85.

(45) Ghaddar, T. H.; Wishart, J. F.; Thompson, D. W.; Whitesell, J. K.; Fox, M. A. *J. Am. Chem. Soc.* **2002**, *124*, 8285.

(46) Lacoste, M.; Rabaâ, H.; Astruc, D.; Ardoin, N.; Varret, F.; Saillard, J.-Y.; Le Beuze, A. *J. Am. Chem. Soc.* **1990**, *112*, 9548.

(47) (a) Valásek, M.; Pecka, J.; Jindrich, J.; Calleja, G.; Craig, P. R.; Michl, J. *J. Org. Chem.* **2005**, *70*, 405. (b) Berlin, Y. A.; Hutchison, G. R.; Rempala, P.; Ratner, M. A.; Michl, J. *J. Phys. Chem. A* **2003**, *107*, 3970. (c) Schwab, P. F. H.; Levin, M. D.; Michl, J. *Chem. Rev.* **1999**, *99*, 1863.

(48) Hromadová, M.; Kolivoska, V.; Gál, M.; Pospísil, L.; Sokolová, R.; Valásek, M. *J. Incl. Phenom. Macrocycl. Chem.* **2011**, *70*, 461.

(49) Namazian, M.; Almodarresieh, H. A.; Noorbala, M. R.; Zare, H. R. *Chem. Phys. Lett.* **2004**, *396*, 424.

(50) Adamo, C.; Barone, V. *J. Chem. Phys.* **1999**, *110*, 6158.

(51) Dunning, T. H.; Hay, P. J. In *Modern Theoretical Chemistry*; Schaefer, H. F., Ed.; Plenum: New York, 1976; pp 1−28.

(52) Yanai, T.; Tew, D.; Handy, N. *Chem. Phys. Lett.* **2004**, *393*, 51.

(53) Miertus, S.; Scrocco, E.; Tomasi, J. *Chem. Phys.* **1981**, *55*, 117.

(54) Scalmani, G.; Frisch, M. J.; Mennucci, B.; Tomasi, J.; Cammi, R.; Barone, V. *J. Chem. Phys.* **2006**, *124*, 094107.

(55) Frisch, M. J. et al. *Gaussian 09*; Gaussian Inc.: Wallingford CT, 2010.

(56) Pavlishchuk, V. V.; Addison, A. W. *Inorg. Chim. Acta* **2000**, *298*, 97.

(57) Krejčík, M.; Danek, M.; Hartl, F. *J. Electroanal. Chem.* **1991**, *317*, 179.

(58) http://www.reading.ac.uk/web/FILES/chemistry/F_Hartl_OTTLE_cells.pdf

(59) http://www.specac.com/products/liquid-transmission-cell/ft-ir-liquidtransmission-cell/530